Classificazione dei Sistemi Dinamici
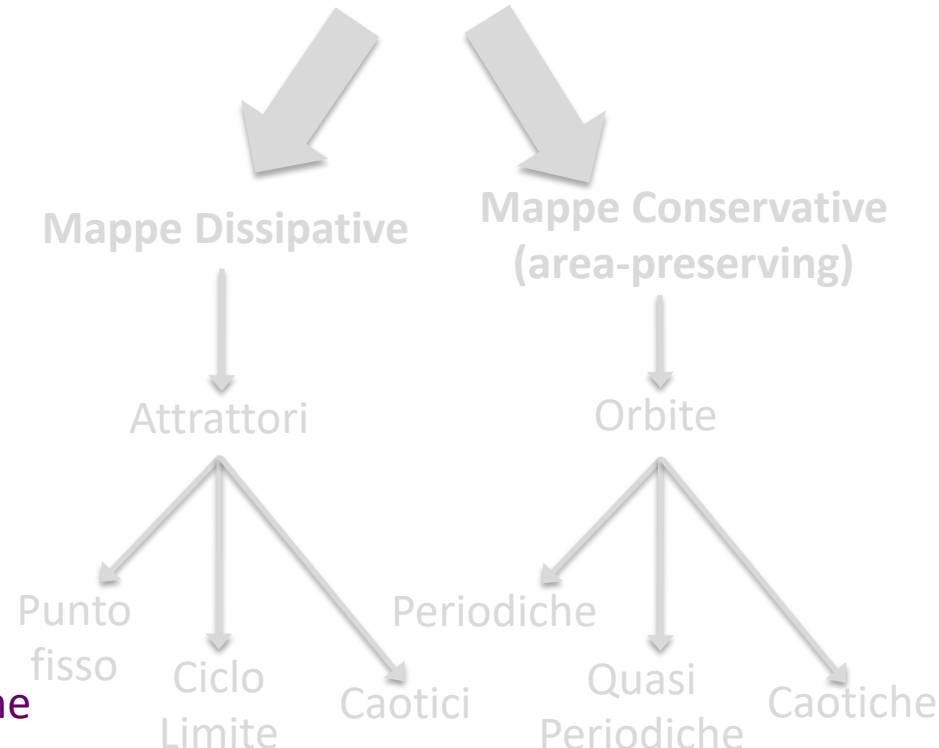
Sistemi dinamici continui (Flussi)

$$\dot{X} = f(X)$$
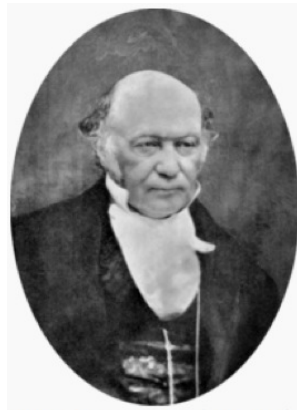
Flussi Dissipativi

Attrattori

1D

2D

3D

Punto fisso

Ciclo Limite

Caotici

Flussi Hamiltoniani

Orbite

Periodiche

Quasi Periodiche

Caotiche

Sistemi dinamici discreti (Mappe)

$$x_{n+1} = A x_n (1 - x_n) \equiv f_A(x)$$

Mappe Dissipative

Attrattori

Punto fisso

Ciclo Limite

Caotici

Mappe Conservative (area-preserving)
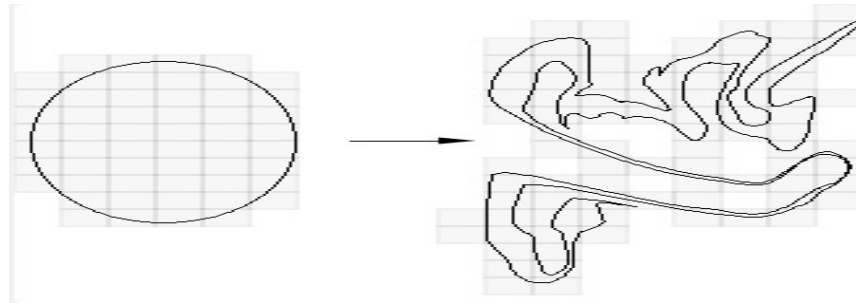
Orbite

Periodiche

Quasi Periodiche

Caotiche

Flussi Hamiltoniani

William Rowan Hamilton (1805–1865)

$$\frac{1}{V}\frac{dV}{dt} = \sum_i \frac{\partial f_i}{\partial x_i} = 0$$

The evolution of the Hamiltonian system is completely described if the time dependence of the qs and ps is known. That is, if we know $q_i(t)$ and $p_i(t)$ for all t and for all i, then we know everything there is to know about the time behavior of the system. In the Hamilton formulation, the time-dependence of the qs and ps is determined by solutions of Hamilton's equations, which are written in terms of the derivatives of the ***Hamiltonian function*** (or just ***Hamiltonian***, for short) $H(q,p)$, where the unadorned symbols q and p mean that H depends, in general, on all the q_i and p_i. For the simplest cases, the Hamiltonian is just the total mechanical energy (kinetic energy plus potential energy) of the system, written as a function of the qs and ps. In any case, Hamilton's equations are a set of $2N$ coupled differential equations (for a system of N degrees of freedom)

Hamilton's Equations

$$\begin{cases} \dfrac{dq_i}{dt} = \dfrac{\partial H(q,p)}{\partial p_i} \\[2mm] \dfrac{dp_i}{dt} = -\dfrac{\partial H(q,p)}{\partial q_i} \end{cases} \quad i = 1,\ldots,N$$

$\equiv$

$$\begin{cases} \dot{q}_i = f_i(q_i,p_i) \\[2mm] \dot{p}_i = g_i(q_i,p_i) \end{cases} \quad i = 1..N$$

Sistema Hamiltoniano ad N gradi di libertà (vive in uno spazio delle fasi a 2N dimensioni)

$$f_i(q_i,p_i) = \frac{\partial H(q_{i,}p_i)}{\partial p_i}$$

$$g_i(q_i,p_i) = -\frac{\partial H(q_{i,}p_i)}{\partial q_i}$$

Since the Hamiltonian function value (usually the energy of the system) is a constant of the motion, a trajectory for a Hamiltonian system cannot go just anywhere in phase space. It can go only to regions of (q, p) space that have the same energy value as the initial point of the trajectory. Thus, we say that trajectories in phase space are confined to a $2N - 1$ dimensional *constant energy surface*. (Of course, this "surface" may be a multidimensional geometric object in general.)
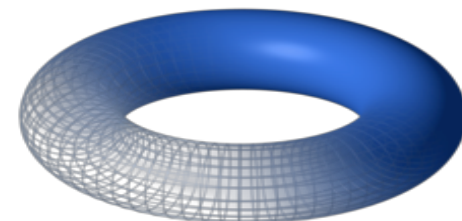
Esempi:

Sistema Hamiltoniano
ad 1 grado di libertà
(2N=2 dimensioni)
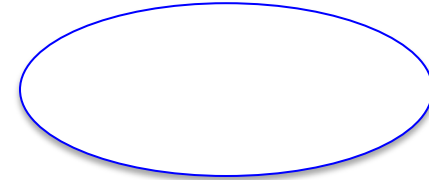
La traiettoria è confinata lungo una linea chiusa 1D (toro unidimensionale), luogo dei punti dello spazio delle fasi ad energia costante

Sistema Hamiltoniano
a 2 gradi di libertà
(2N=4 dimensioni)

La traiettoria è confinata nel volume 3D di un toro, ipersuperficie ad energia costante

Sistemi Integrabili

The special case we are interested in is a canonical transformation that leads to a Hamiltonian that depends only on the J_is and not on the θ_is. In that case, for all $i = 1, 2, \ldots, N$, we have

azione   angolo

$$H = H(J) \;\rightarrow\; \dot{J_i} = 0 \;;\; \theta_i(t) = \omega_i t + \theta_i(0)$$

$$\dot{\theta_i} = \frac{\partial H(\theta, J)}{\partial J_i}$$

$$\dot{J_i} = -\frac{\partial H(\theta, J)}{\partial \theta_i}$$

and the J_is are the N constants of the motion.

A Hamiltonian system that satisfies Eqs. (8.4-3) and (8.4-4) is called (somewhat unfortunately) an **integrable system**. The term *integrable* comes from the notion that the action J_i can be expressed as an integral over the motion of the system and that the corresponding equation for θ_i can be easily integrated.

1. All one-degree-of-freedom Hamiltonian systems, for which H is an infinitely differentiable (that is, "analytic") function of q and p, are integrable and the corresponding action J satisfies $H = \omega\, J$, where $\omega = \partial H/\partial J$.

2. All Hamiltonian systems for which Hamilton's equations are linear in q and p are integrable (via the so-called normal mode transformations).

3. All Hamiltonian systems with nonlinear Hamilton's equations that can be separated into uncoupled one-degree-of-freedom systems are integrable.

Flussi Hamiltoniani
ad un grado di libertà

We will now study two examples of one-degree-of-freedom Hamiltonian systems and their phase space behavior.
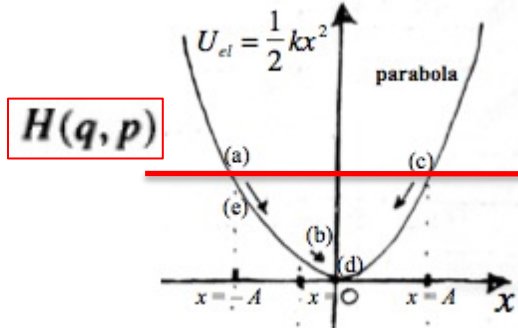
The Simple Harmonic Oscillator

In Exercise 8.2-2, we learned that the Hamiltonian for a one-dimensional simple harmonic oscillator with mass m and spring constant k is
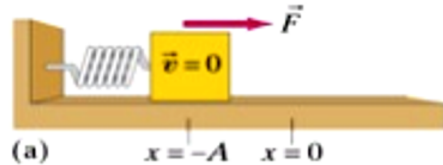
$$H(q,p) = \frac{p^2}{2m} + \tfrac{1}{2}kq^2 \qquad (8.4\text{-}8)$$

where q is the displacement of the oscillator from its equilibrium position. In this case, the numerical value of the Hamiltonian is the total mechanical energy of the system. The corresponding Hamilton's equations for the time evolution are

$H(q,p)$

$$\begin{cases} \dot{q} = \dfrac{\partial H}{\partial p} = \dfrac{p}{m} \\[2mm] \dot{p} = -\dfrac{\partial H}{\partial q} = -kq \end{cases}$$

$$\ddot{q}(t) = \frac{\dot{p}(t)}{m} = -\frac{k}{m}q(t)$$

Punto fisso: q=0, p=0

The one (spatial) dimension simple harmonic oscillator model has one degree of freedom and its phase space is two-dimensional. Since the Hamiltonian is independent of time, the phase space trajectories must reside on a $2N-1 = 1$ dimensional "surface" (i.e., on a curve). The trajectories are closed curves because the motion is periodic. Each value of the energy is associated with a unique closed curve.

For the simple harmonic oscillator, we know that the angular frequency of the oscillatory motion is given by $\omega = \sqrt{k/m}$. Since this is a one-degree-of-freedom system or since Hamilton's equations are linear, we expect that this system is integrable. The one constant of the motion is the Hamiltonian (energy) or some multiple thereof. Hence, we can write the action J as

$$\boxed{H = \omega\, J} \longrightarrow J = \frac{H}{\omega} = \frac{p^2}{2m\omega} + \frac{kq^2}{2\omega} \qquad (8.4\text{-}10)$$

p

q

punto ellittico

If we use $p/\sqrt{2m\omega}$ and $q\sqrt{m\omega/2}$ as the phase space variables, then the trajectories will be circles with radii equal to $\sqrt{J}$. To complete the story, we can write the original phase space variables p and q in terms of the action-angle variables (with θ positive going counterclockwise from the positive q axis):

p'

$\sqrt{J}$

θ

q'

$\theta(t) = \omega t + \theta(0)$

$$\boxed{\begin{cases} p(t) = \sqrt{2m\omega J}\,\sin\theta(t) \\ q(t) = \sqrt{2J/(m\omega)}\,\cos\theta(t) \end{cases} \rightarrow \begin{cases} p'(t) = \sqrt{J}\,\sin\theta(t) \\ q'(t) = \sqrt{J}\,\cos\theta(t) \end{cases}} \qquad (8.4\text{-}11)$$
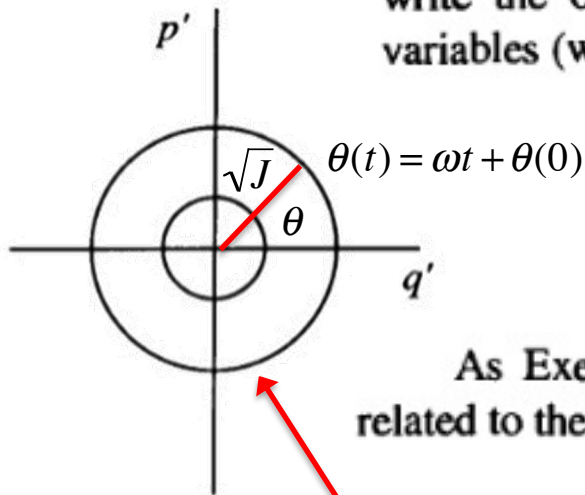
As Exercise 8.4-1 shows, the action associated with a closed trajectory is related to the phase space area enclosed by the trajectory. In general, we may write

$$J = \frac{1}{2\pi}\oint p\,dq \qquad (8.4\text{-}12)$$
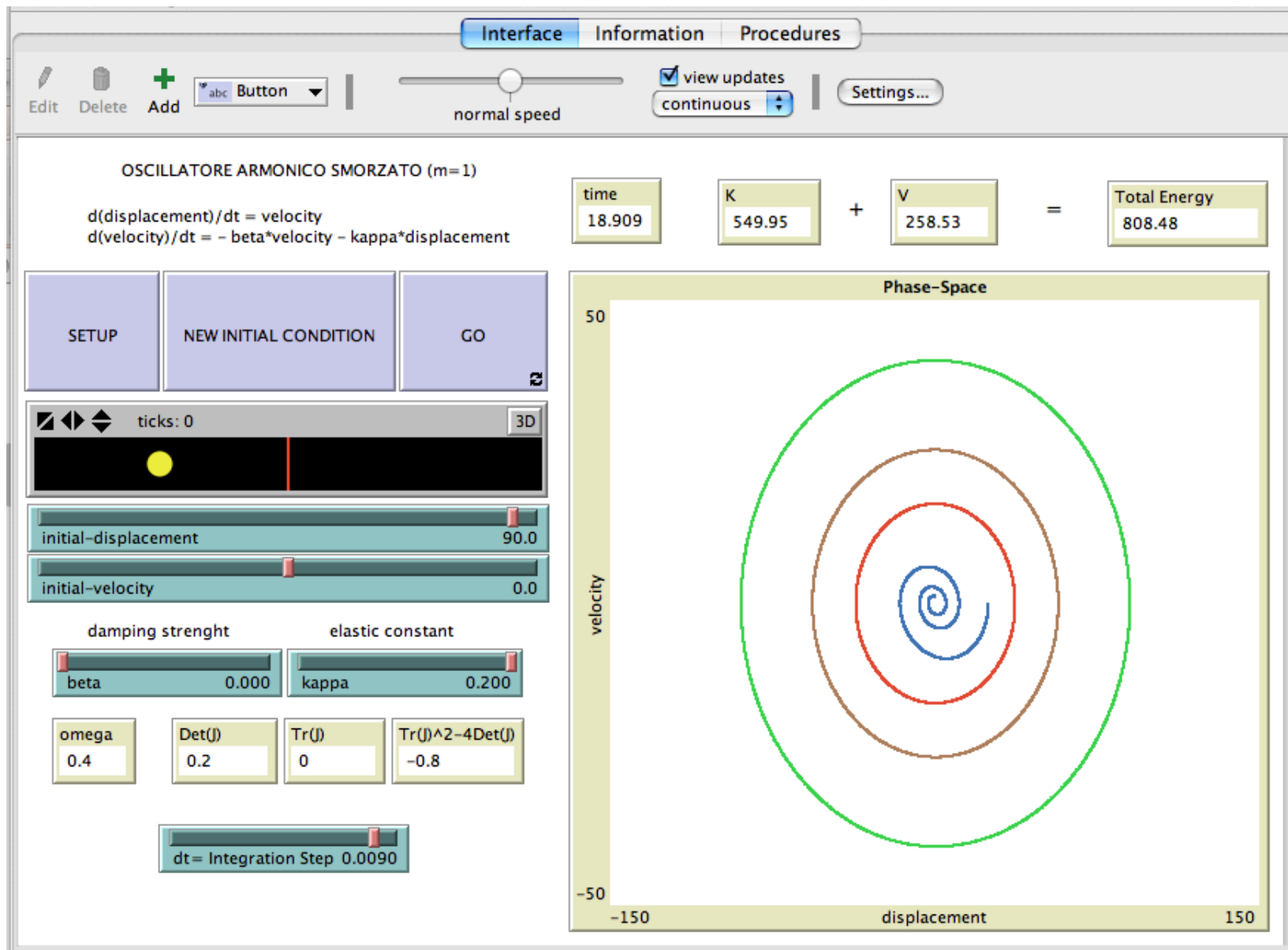
where the symbol $\oint$ means that the integral is taken around the closed path of the trajectory.
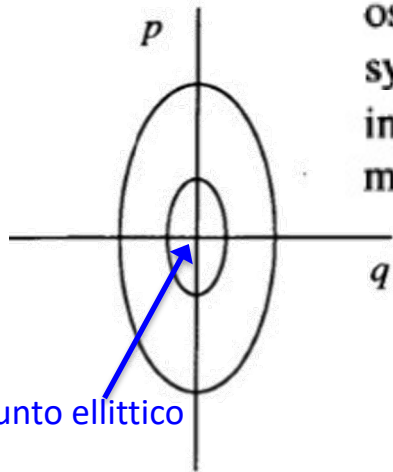
oscillatore-armonico.nlogo

Oscillatore Armonico non Smorzato

Oscillatore Armonico Smorzato

$$\begin{cases} \dot{q} = p \quad (m = 1) \\ \dot{p} = -kq \end{cases}$$

$$\begin{cases} \dot{q} = p \quad (m = 1) \\ \dot{p} = -bp - kq \end{cases}$$
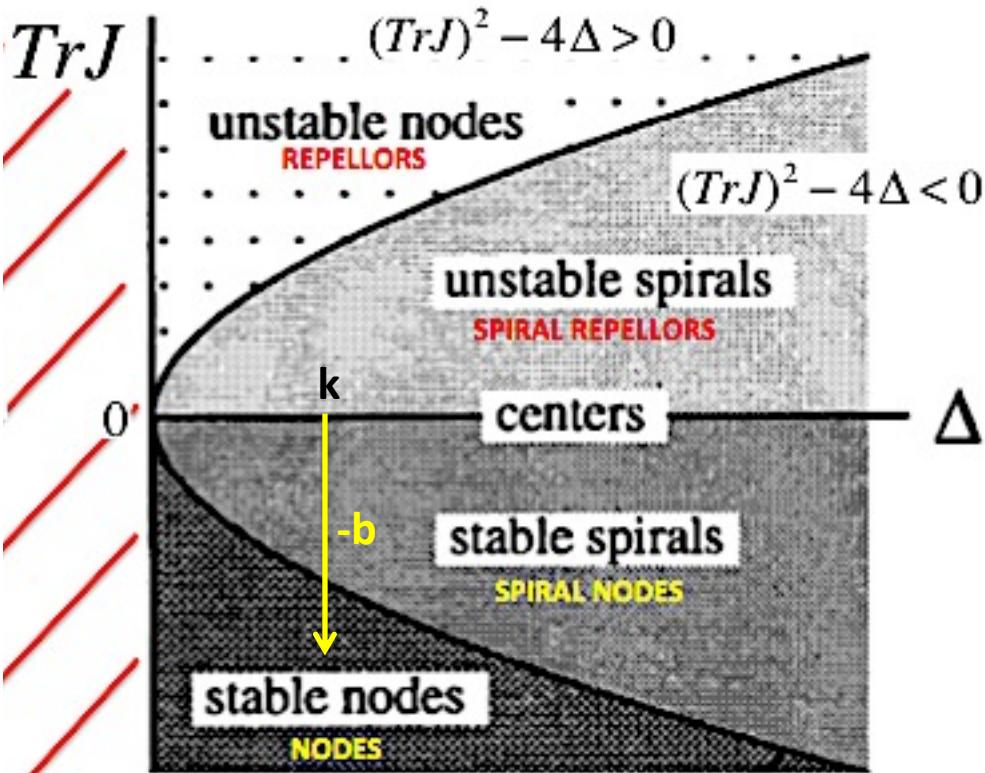
$$\ddot{q} + kq = 0$$

$$\ddot{q} + b\dot{q} + kq = 0$$

Punto Ellittico:

$$q = 0 \ , \ p = 0$$

Attrattore a punto fisso:

$$q = 0 \ , \ p = 0$$

WolframAlpha

`{{0,1},{-k,-b}}`

Input:

$$\begin{pmatrix} 0 & 1 \\ -k & -b \end{pmatrix} \qquad J = \begin{pmatrix} f_{11} & f_{12} \\ f_{21} & f_{22} \end{pmatrix}$$

Dimensions:

2 (rows) $\times$ 2 (columns)

Determinant:

k

Trace:

$-b$

Characteristic polynomial:

$b\,x + k + x^2$

Eigenvalues:

$$\lambda_1 = \frac{1}{2}\left(-\sqrt{b^2 - 4k} - b\right)$$

$$\lambda_2 = \frac{1}{2}\left(\sqrt{b^2 - 4k} - b\right)$$

Il Pendolo Conservativo

One of the most studied and time-honored examples of a Hamiltonian system is the pendulum. This system consists of a point mass m suspended at the end of a rigid (but massless) rod of length L. The rod is free to pivot about an axis at the other end of the rod. To make the system Hamiltonian, we ignore any dissipation due to friction in the pivot or to air resistance. A picture of this system is shown in Fig. 8.2.

The Hamiltonian for this system is expressed as the sum of kinetic energy of rotation about the pivot point and gravitational potential energy (relative to the equilibrium point when the pendulum mass hangs downward):
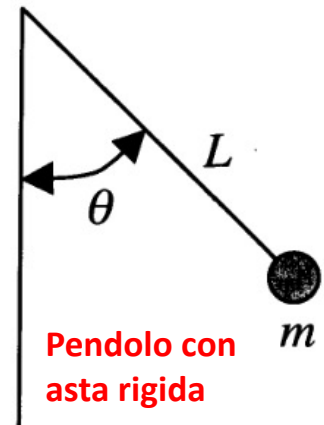
$$H = \frac{p_\theta^2}{2mL^2} + mgL(1 - \cos\theta) \qquad (8.4\text{-}13)$$

where p_θ is the angular momentum associated with the rotation about the axis and g is the acceleration due to gravity. Thus, we see that the pendulum is a one-degree-of-freedom system (with a two-dimensional phase space). Hence, by the arguments presented earlier, it is an integrable system with one constant of the motion, namely its total mechanical energy E.
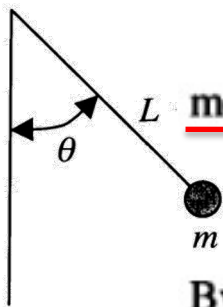
Eq. di Hamilton

Fig. 8.2. A picture of the pendulum. The angle θ is defined relative to the stable equilibrium position. Gravity acts downward.

$$\begin{cases} \dot{\theta} = \dfrac{\partial H}{\partial p_\theta} = \dfrac{p_\theta}{mL^2} \\[3mm] \dot{p}_\theta = -\dfrac{\partial H}{\partial \theta} = -mgL\sin\theta \end{cases}$$

$$\longrightarrow \qquad \ddot{\theta} = \frac{\dot{p}_\theta}{mL^2} = -\frac{g}{L}\sin\theta$$
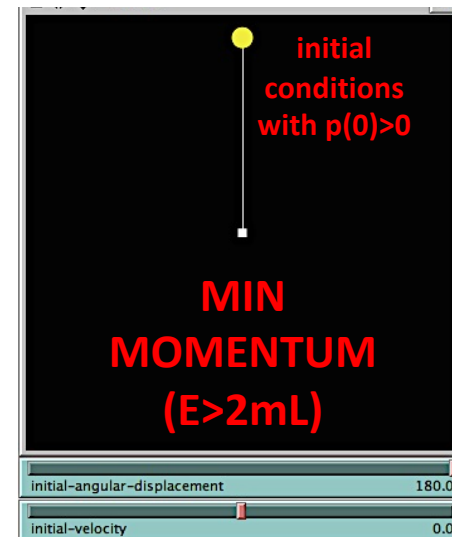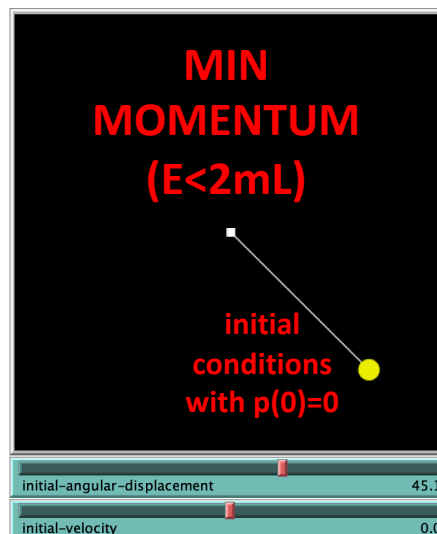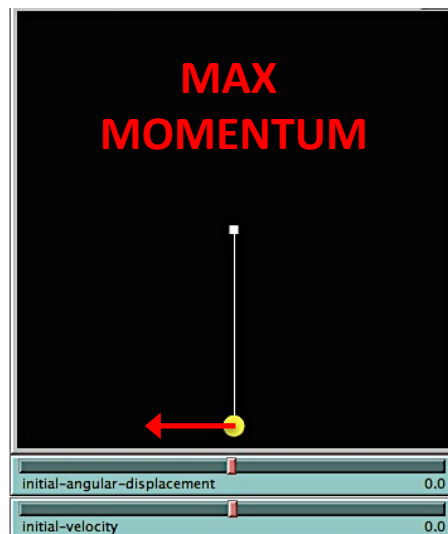
L

θ

Pendolo con asta rigida

m

For a given value of the energy E, we can use Eq. (8.4-13) to solve for the momentum

$$p_\theta = \pm\sqrt{2mL^2[E - mgL(1 - \cos\theta)]} \qquad (8.4\text{-}14)$$

By convention, the momentum is positive when the pendulum is moving counterclockwise and negative when the pendulum is moving clockwise. From Eq. (8.4-14), we see that the momentum has its largest magnitude when $\theta = 0$, at the bottom of the pendulum's swing. For energies less than $2mgL$, the highest point of the swing occurs when $p_\theta = 0$ or in terms of the angular displacement from the vertical line, when $E = mgL(1 - \cos\theta)$. If we allow the pendulum to swing over the top by giving it sufficient energy (greater than $2mgL$), then the minimum of its momentum magnitude occurs when $\theta = \pi$ at the top of the swing. Eq. (8.4-14) can be used to plot the phase space trajectories as shown in Fig. 8.3.

For a given value of the energy E, we can use Eq. (8.4-13) to solve for the momentum

$$p_\theta = \pm\sqrt{2mL^2[E - mgL(1 - \cos\theta)]} \qquad (8.4\text{-}14)$$

By convention, the momentum is positive when the pendulum is moving counterclockwise and negative when the pendulum is moving clockwise. From Eq. (8.4-14), we see that the momentum has its largest magnitude when $\theta = 0$, at the bottom of the pendulum's swing. For energies less than $2mgL$, the highest point of the swing occurs when $p_\theta = 0$ or in terms of the angular displacement from the vertical line, when $E = mgL(1 - \cos\theta)$. If we allow the pendulum to swing over the top by giving it sufficient energy (greater than $2mgL$), then the minimum of its momentum magnitude occurs when $\theta = \pi$ at the top of the swing. Eq. (8.4-14) can be used to plot the phase space trajectories as shown in Fig. 8.3.

We can find the corresponding action J for the system by integrating the momentum over one cycle of the motion

$$J = \frac{1}{2\pi}\int d\theta \sqrt{2mL^2[E - mgL(1 - \cos\theta)]} \qquad (8.4\text{-}15)$$

The resulting integral is known as an *elliptic integral* and is tabulated numerically in many mathematical handbooks. The important point here is that we can determine the frequency of the motion, numerically, by using Eq. (8.4-15) with Eq. (8.4-5).

$$\dot{\theta}_i = \frac{\partial H}{\partial J_i} \equiv \omega_i(J) \rightarrow \omega = \frac{H}{J}$$

pendolo-conservativo.nlogo
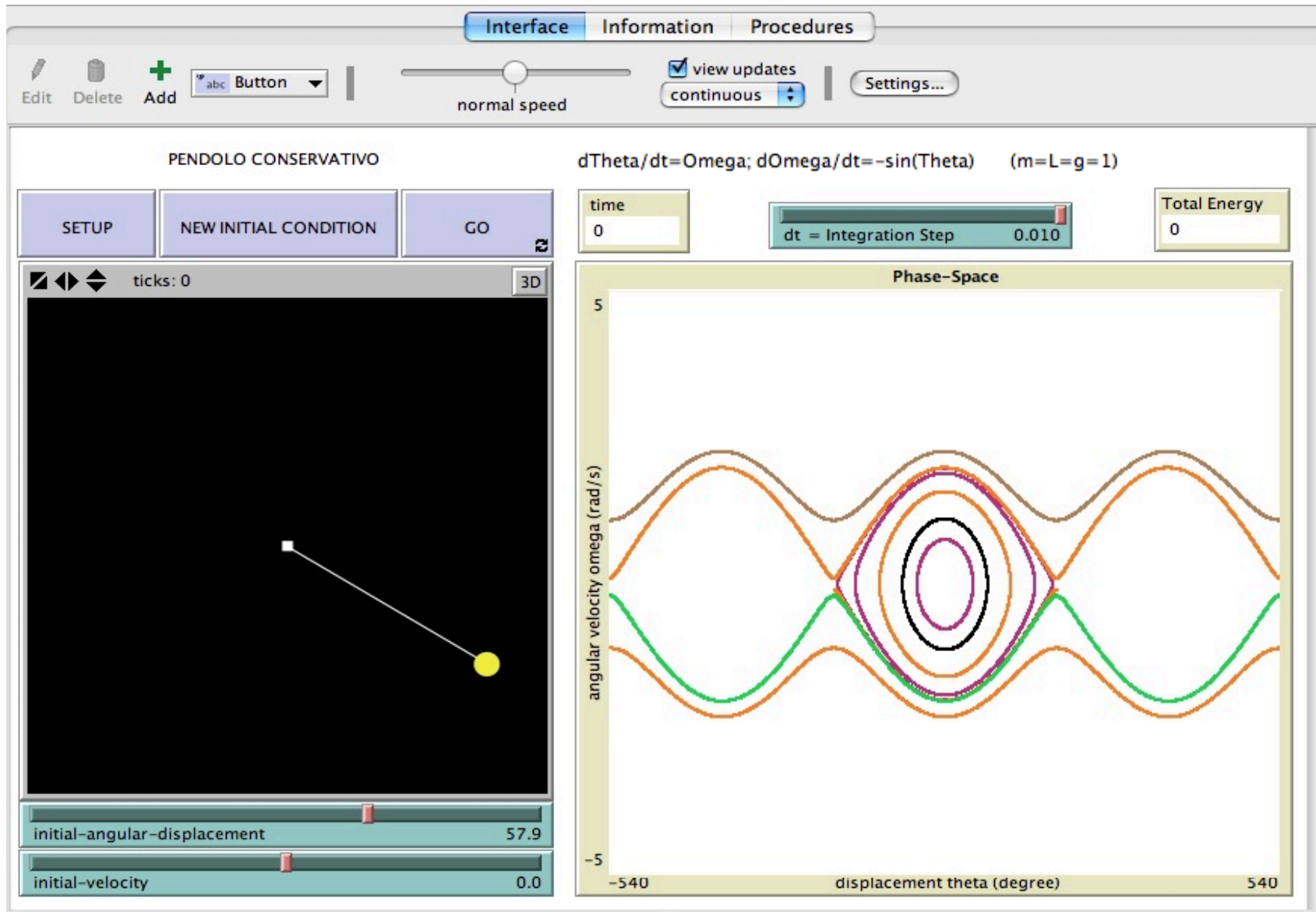
Spazio delle Fasi 2D del Pendolo Conservativo (m=g=L=1)

The phase space diagram for the pendulum, shown in Fig. 8.3, is typical of the phase space diagrams for many integrable Hamiltonian systems. For relatively small values of the energy, the phase space trajectories are "ellipses" centered on the origin. At the origin is an elliptic fixed point for the system: If the system starts with $p_\theta = 0$ and $\theta = 0$, then it stays there for all time. These ellipses are the "tori" on which the trajectories live in this two-dimensional phase space.

Eq. di Hamilton

$$\begin{cases} \dot{\theta} = \dfrac{\partial H}{\partial p_\theta} = p_\theta \\[2mm] \dot{p}_\theta = -\dfrac{\partial H}{\partial \theta} = -\sin\theta \end{cases}$$
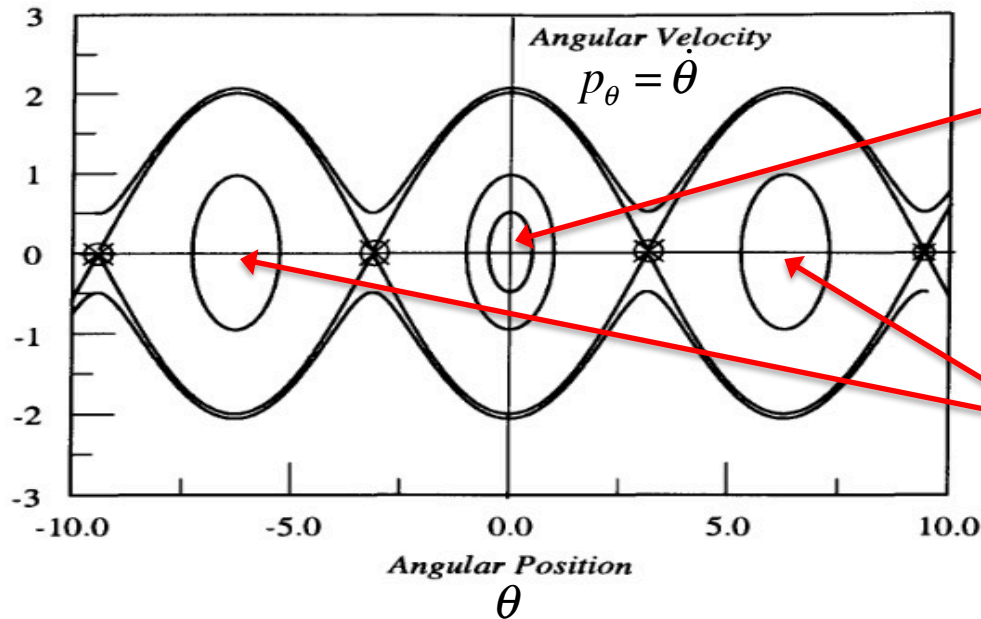
$$J \equiv \begin{pmatrix} 0 & 1 \\ -\cos\theta & 0 \end{pmatrix}$$

Punto fisso "ellittico" nell'origine

$$\theta = 0 \ , \ p_\theta = 0$$

Altri punti fissi ellittici

$$\theta = \pm 2n\pi \ , \ p_\theta = 0$$

$$\theta = \pm 2n\pi \ , \ p_\theta = 0$$

$$J \equiv \begin{pmatrix} 0 & 1 \\ -1 & 0 \end{pmatrix}$$
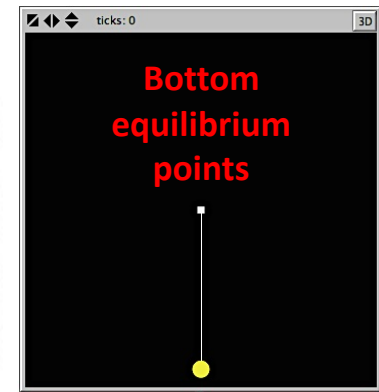
$$Det J = 1 > 0$$

$$Tr J = 0$$

Fig. 8.3. The phase diagram for the pendulum. Angular velocity (vertical axis) is plotted as a function of angular position (horizontal axis). Each trajectory corresponds to a particular value of the total mechanical energy of the system. Elliptic fixed points occur at the origin and at angular positions of $\pm n2\pi$ for positive or negative integer n. Hyperbolic (saddle) points occur at $\theta = \pm\pi$. These are indicated by small circles. The trajectories that join the hyperbolic points are separatrices. Inside the separatrices, the motion is periodic and oscillatory. The motion on trajectories outside the separatrices corresponds to counterclockwise revolutions for $\dot{\theta} > 0$ and clockwise revolutions for $\dot{\theta} < 0$.

Bottom equilibrium points

The phase space diagram for the pendulum, shown in Fig. 8.3, is typical of the phase space diagrams for many integrable Hamiltonian systems. For relatively small values of the energy, the phase space trajectories are "ellipses" centered on the origin. At the origin is an elliptic fixed point for the system: If the system starts with $p_\theta = 0$ and $\theta = 0$, then it stays there for all time. These ellipses are the "tori" on which the trajectories live in this two-dimensional phase space.

Eq. di Hamilton

$$\begin{cases} \dot{\theta} = \dfrac{\partial H}{\partial p_\theta} = p_\theta \\[2ex] \dot{p}_\theta = -\dfrac{\partial H}{\partial \theta} = -\sin\theta \end{cases}$$
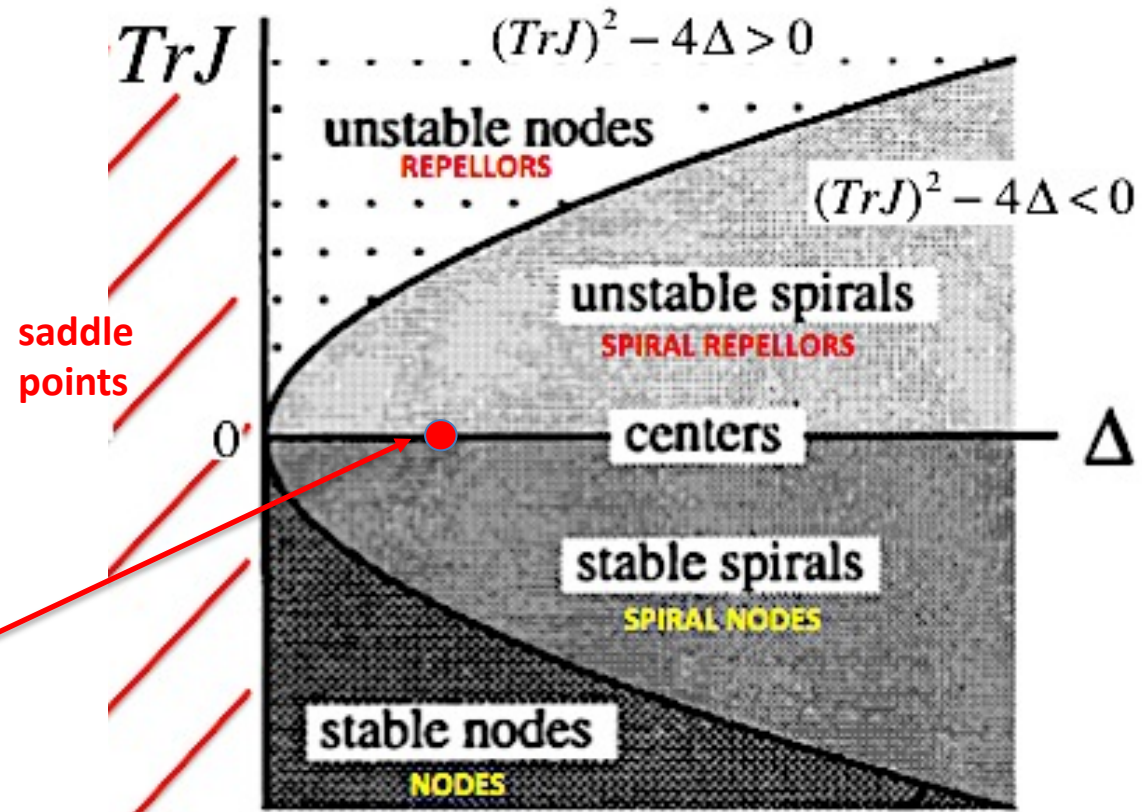
$$J \equiv \begin{pmatrix} 0 & 1 \\ -\cos\theta & 0 \end{pmatrix}$$

$$\theta = \pm 2n\pi \ , \ p_\theta = 0$$

$$J \equiv \begin{pmatrix} 0 & 1 \\ -1 & 0 \end{pmatrix}$$

$$DetJ = 1 > 0$$

$$TrJ = 0$$

TrJ

$(TrJ)^2 - 4\Delta > 0$

unstable nodes
REPELLORS

$(TrJ)^2 - 4\Delta < 0$

unstable spirals
SPIRAL REPELLORS

saddle points

0

centers Δ

stable spirals
SPIRAL NODES

stable nodes
NODES

There are also fixed points at $p_\theta = 0$ and $\theta = \pm n\pi$, where n is an odd integer. These fixed points correspond to the pendulum's standing straight up with the mass directly above the pivot point. Note that $\theta = \pm\pi$ are physically equivalent points since they both correspond to the vertical position of the pendulum. However, it is occasionally useful to allow the angle to increase or decrease without limit to visualize some aspects of the pendulum's motion. The physical equivalence shows up in the periodicity of the trajectory pictures in state space if you shift along the θ axis by multiples of 2π.

The fixed points corresponding to the inverted vertical position are unstable in the sense that the slightest deviation from those conditions causes the pendulum to swing away from the inverted vertical position. These fixed points are called **hyperbolic points** for Hamiltonian systems because trajectories in their neighborhood look like hyperbolas. The fixed points are, of course, saddle points using the terminology introduced in Chapter 3. Trajectories approach the hyperbolic point in one direction and are repelled in another direction.

$$J \equiv \begin{pmatrix} 0 & 1 \\ -\cos\theta & 0 \end{pmatrix}$$
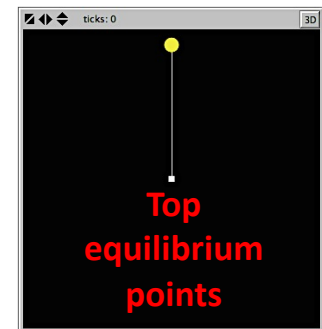
$$\theta = \pm(2n+1)\pi, p_\theta = 0$$

$$J \equiv \begin{pmatrix} 0 & 1 \\ 1 & 0 \end{pmatrix}$$

$$DetJ = -1 < 0$$
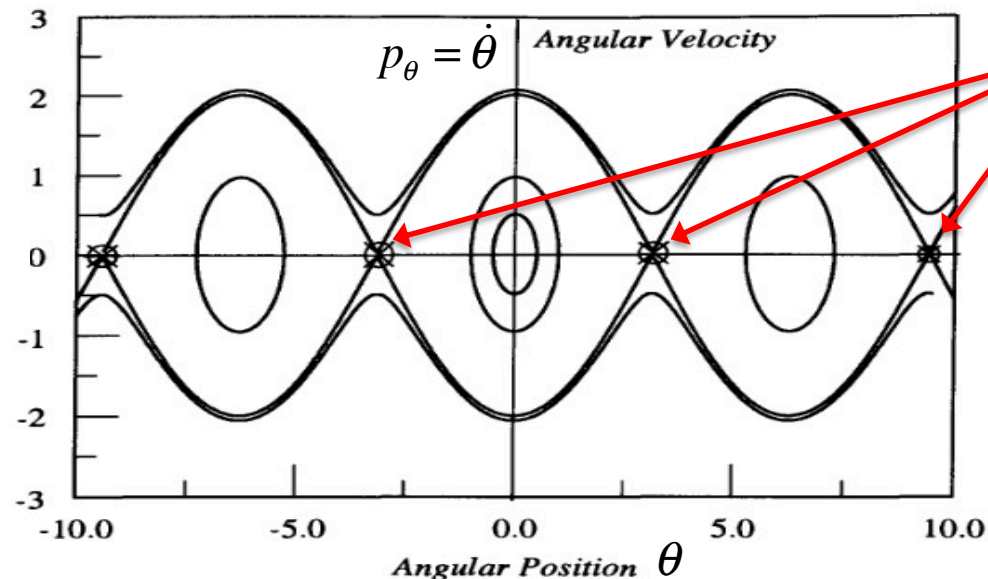
Punti fissi "iperbolici" (saddle points)

$$\theta = \pm(2n+1)\pi, p_\theta = 0$$

Top equilibrium points

$p_\theta = \dot\theta$ — Angular Velocity

Angular Position θ

The trajectories that lead directly to or directly away from a hyperbolic point are called *separatrices* (plural of *separatrix*) since they separate the phase space into regions of qualitatively different behavior. (The separatrices are the stable and unstable manifolds introduced before.) For the pendulum, the trajectories inside the separatrices correspond to oscillatory motion about the vertically downward equilibrium point. Trajectories outside the separatrices correspond to "running modes" in which the pendulum has sufficient energy to swing over the top. One type of running mode has an angular velocity that is positive (counterclockwise motion); the other type has a negative angular velocity (clockwise motion). In both cases, the magnitude of the angle θ continues to increase with time.

This organization of the phase space by elliptic points surrounded by the separatrices associated with hyperbolic points is typical for integrable Hamiltonian systems. The separatrices segregate phase space regions that correspond to qualitatively different kinds of motion.

Separatrici

Separatrici
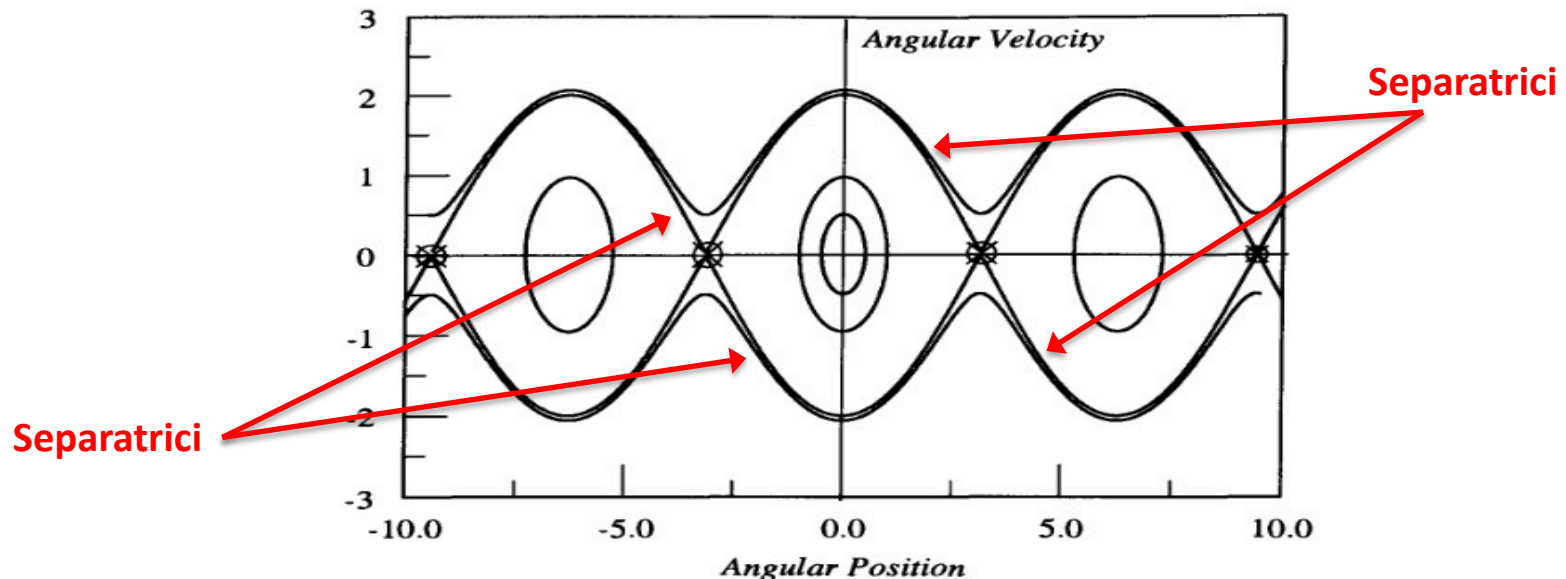
Il Pendolo Forzato-Smorzato

L'equazione piú generale che descrive un pendolo costituito da una massa m appesa ad un filo inestensibile di lunghezza L e soggetto alla forza gravitazionale, ad una forza di smorzamento (damping) e ad una forzante esterna (driving), é quella del cosiddetto 'pendolo forzato':

$$mL^2\ddot{\theta} + b\dot{\theta} + mgLsin\theta = k' \cdot cos\ \omega_D t \qquad (1.1)$$

dove θ é la fase del pendolo (ossia il suo spostamento angolare dalla posizione di equilibrio), g l'accelerazione di gravitá, b l'intensitá dello smorzamento e $G = k' \cdot cos\ \omega_D t$ la forzante esterna di intensitá k' e frequenza di *driving* ω_D. Attraverso una opportuna scelta dei parametri e riscalando l'unitá di tempo é possibile riscrivere l'equazione 1.1 nella sua forma adimensionale [4]:

$$\ddot{\theta} + \beta\dot{\theta} + sin\theta = k \cdot cos\ \omega_D t \qquad (1.2)$$

dove β é il nuovo coefficiente di smorzamento e $\Gamma = k \cdot cos\ \omega_D t$ la forzante di intensitá k. A questo punto, in funzione dei valori che puó assumere il parametro β, possiamo descrivere la dinamica del pendolo forzato dividendola in due categorie fondamentali: per valori positivi di β abbiamo la versione *dissipativa*, che presenta svariati punti di contatto (ma anche di divergenza) con quanto visto nel caso delle mappe dissipative, mentre per valori nulli di β abbiamo la versione *conservativa*, che ci permetterá di introdurre nuovi interessanti concetti sui sistemi dinamici.

pendolo-forzato-smorzato.nlogo
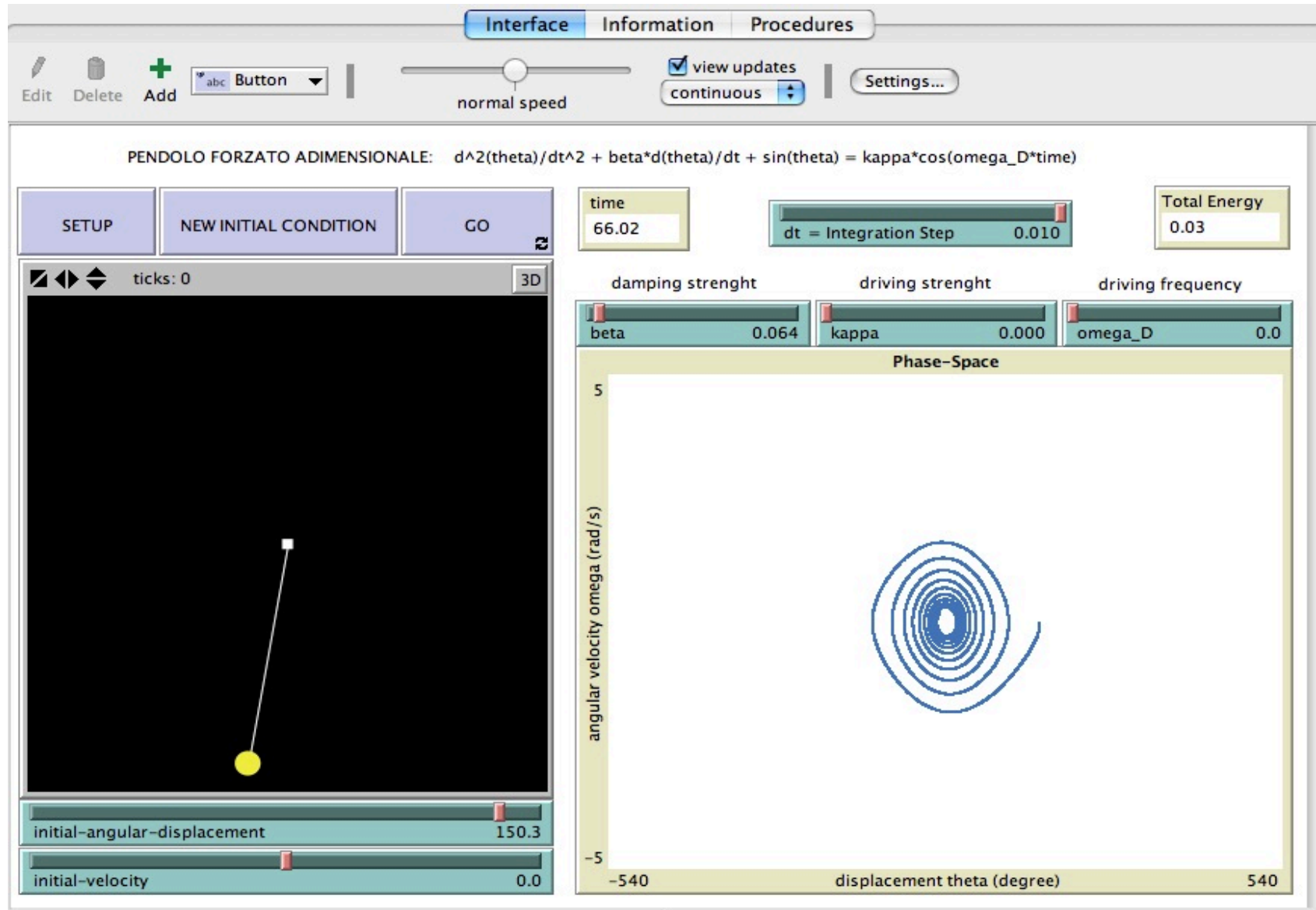
1.2.1 Caso Dissipativo ($\beta > 0$)

Per valori di $\beta > 0$, ossia per valori positivi del coefficiente di smorzamento, l'eq.1.1 descrive un sistema dissipativo, la cui energia totale non si conserva nel tempo: in questo caso, analogamente a quanto abbiamo visto accadere per le mappe dissipative studiate nei capitoli precedenti, l'evoluzione asintotica del sistema non dipende dalle condizioni iniziali e converge verso particolari configurazioni nello spazio delle fasi, ossia verso i cosiddetti *attrattori* della dinamica. In questo caso peró il tipo di attrattori verso i quali puó convergere un sistema dinamico continuo dipende fortemente dal suo numero n di gradi di libertá: infatti per $n = 1$ sono possibili solo attrattori a *punto fisso*, per $n = 2$ si aggiungono attrattori a *ciclo limite*, mentre solo per $n \geq 3$ diventa possibile osservare quelli che in precedenza abbiamo chiamato attrattori strani, cioé *attrattori caotici*. La spiega-
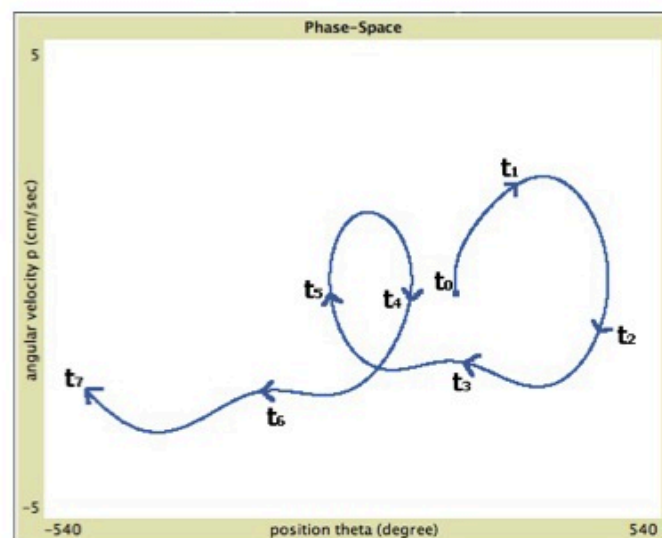

Figura 1.1: Ritratto nello spazio delle fasi dell'evoluzione temporale (traiettoria) di un pendolo forzato e smorzato (vedi testo).

Per poter andare avanti nella trattazione del pendolo forzato occorre quindi rispondere immediatamente alla domanda: quante dimensioni possiede il suo spazio delle fasi? Guardando la Fig.1.1 saremmo tentati di rispondere 'due', ma il lettore attento, osservando la traiettoria rappresentata, dedurrá subito che la risposta corretta non puó essere questa: se cosí fosse infatti, a causa dei teoremi sopra esposti, la traiettoria non potrebbe autointersecarsi. Poiché invece si osserva una autointersezione l'unica possibilitá é che la curva rappresentata in figura sia solamente la proiezione bidimensionale della traiettoria originale la quale quindi, evidentemente, vive in uno spazio ad un numero maggiore di dimensioni. Ma quante (e quali) sono queste dimensioni?
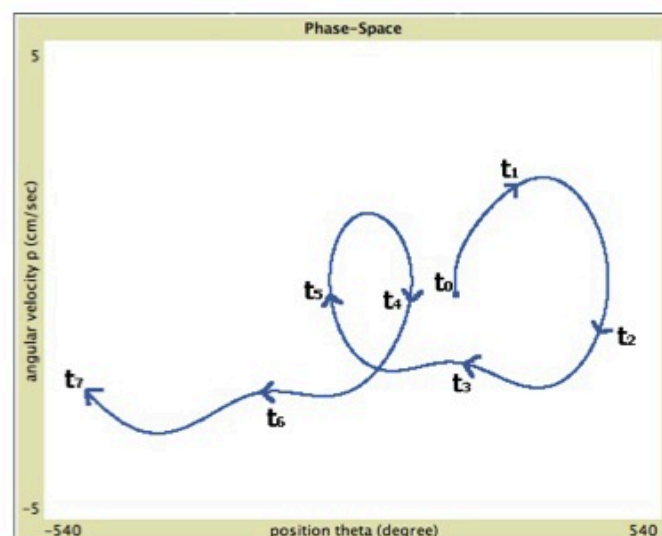

Figura 1.1: Ritratto nello spazio delle fasi dell'evoluzione temporale (traiettoria) di un pendolo forzato e smorzato (vedi testo).

$$\ddot{\theta} + \beta\dot{\theta} + sin\theta = k \cdot cos\ \omega_D t \qquad (1.2)$$

Per scoprirlo torniamo all'equazione 1.2 e, seguendo l'approccio utilizzato nell'introduzione, cerchiamo di trasformarla in un sistema di equazioni accoppiate del primo ordine. A questo scopo conviene riscriverla nel modo seguente:

$$\dot{\omega} = -\beta\omega - sin\theta + k \cdot cos\ \omega_D t \qquad (1.3)$$

dove si é introdotta la velocitá angolare del pendolo $\omega = \dot{\theta}$, da distinguere dalla frequenza di driving ω_D che sará invece data dalla derivata prima della *fase di driving* Φ (definita come $\Phi = \omega_D t$). Considerando assieme le tre equazioni:

$$\begin{cases} \dot{\theta} = \omega \\ \dot{\omega} = -\beta\omega - sin\theta + k \cdot cos\ \Phi \end{cases}$$

Flusso dissipativo 2D non autonomo

$$\ddot{\theta} + \beta\dot{\theta} + sin\theta = k \cdot cos\ \omega_D t \qquad (1.2)$$

Per scoprirlo torniamo all'equazione 1.2 e, seguendo l'approccio utilizzato nell'introduzione, cerchiamo di trasformarla in un sistema di equazioni accoppiate del primo ordine. A questo scopo conviene riscriverla nel modo seguente:

$$\dot{\omega} = -\beta\omega - sin\theta + k \cdot cos\ \omega_D t \qquad (1.3)$$

dove si é introdotta la velocitá angolare del pendolo $\omega = \dot{\theta}$, da distinguere dalla frequenza di driving ω_D che sará invece data dalla derivata prima della *fase di driving* Φ (definita come $\Phi = \omega_D t$). Considerando assieme le tre equazioni:

$$\begin{cases} \dot{\theta} = \omega \\ \dot{\omega} = -\beta\omega - sin\theta + k \cdot cos\ \Phi \\ \dot{\Phi} = \omega_D \end{cases}$$

Flusso dissipativo 3D autonomo

si ottiene proprio il sistema di equazioni cercato, che per $\beta > 0$ rappresenta la dinamica del pendolo forzato dissipativo, il quale rivela quindi la sua natura di sistema dinamico a tre gradi di libertá (θ, ω, Φ), dove tipicamente $\theta \in (-\pi, \pi)$, $\omega \in (-5, 5)$ e $\Phi \in (0, 2\pi)$.

Diagramma di biforcazione per il pendolo forzato-smorzato
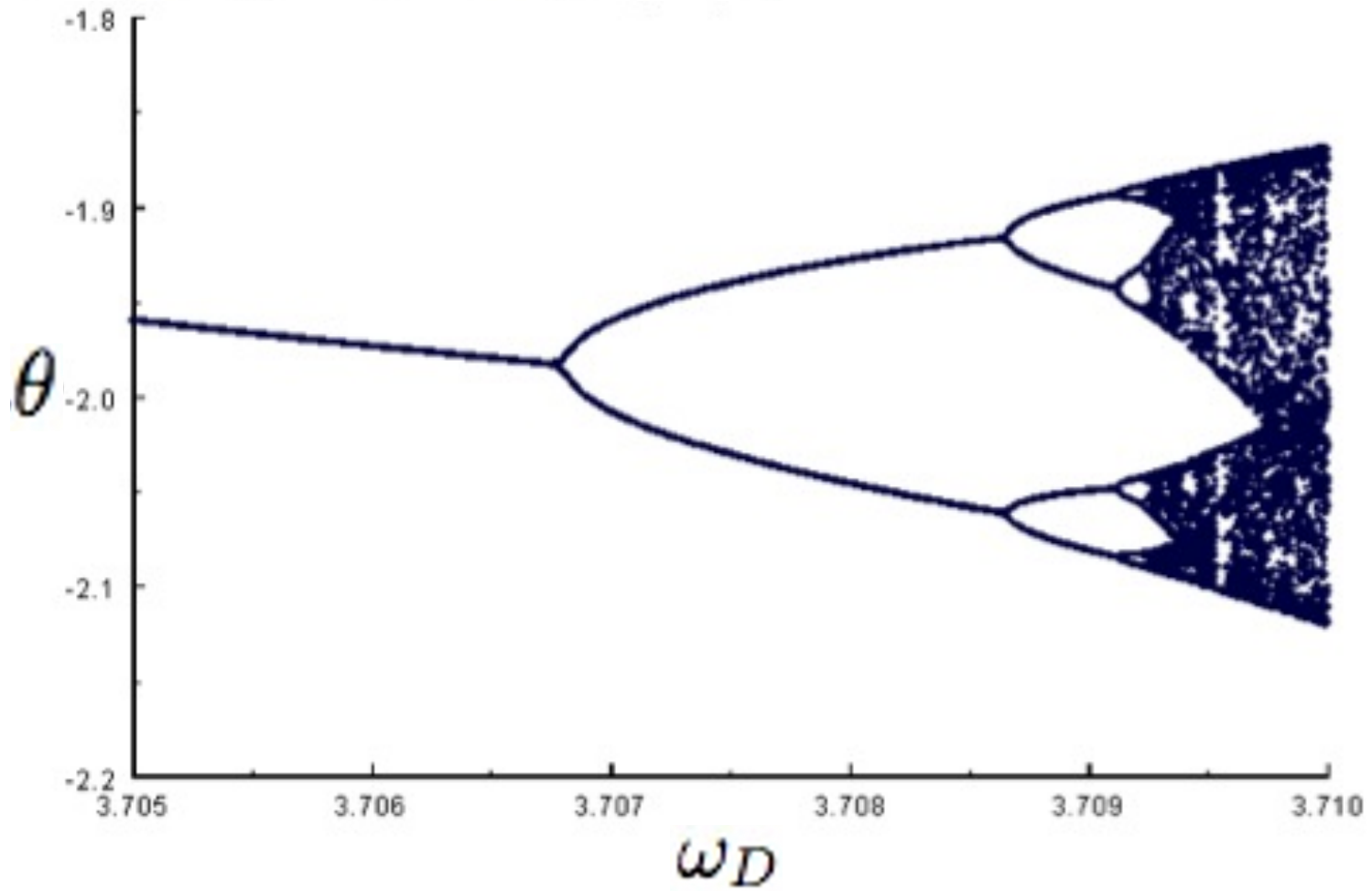
Flussi Hamiltoniani a più gradi di libertà: rotte verso il caos

Systems with N Degrees of Freedom

If we compare Eqs. (8.4-5) and (8.4-6) with the results of the simple harmonic oscillator example, we see that _an integrable system with N degrees of freedom is equivalent, in terms of action-angle variables, to a set of N uncoupled oscillators._ (The oscillators are simple harmonic if the ω_i are independent of the value of the Js. They are otherwise nonlinear oscillators for which ω depends on J.) This connection explains why so much attention is paid to oscillating systems in the study of dynamics.

N gradi di libertà

$$\dot{\theta}_i = \frac{\partial H(\theta, J)}{\partial J_i}$$

$$\dot{J}_i = -\frac{\partial H(\theta, J)}{\partial \theta_i}$$

Azione: $\dot{J}_i = 0 \rightarrow H = H(J_i)$

$$\dot{\theta}_i = \frac{\partial H}{\partial J_i} \equiv \omega_i(J) \qquad i = 1,\ldots,N \qquad \text{(8.4-5)}$$

Angolo: $\theta_i(t) = \omega_i t + \theta_i(0)$ \qquad (8.4-6)

Systems with N Degrees of Freedom

If we compare Eqs. (8.4-5) and (8.4-6) with the results of the simple harmonic oscillator example, we see that an integrable system with N degrees of freedom is equivalent, in terms of action-angle variables, to a set of N uncoupled oscillators. (The oscillators are simple harmonic if the ω_i are independent of the value of the Js. They are otherwise nonlinear oscillators for which ω depends on J.) This connection explains why so much attention is paid to oscillating systems in the study of dynamics.

1 grado di libertà

For the simple harmonic oscillator, we know that the angular frequency of the oscillatory motion is given by $\omega = \sqrt{k/m}$. Since this is a one-degree-of-freedom system or since Hamilton's equations are linear, we expect that this system is integrable. The one constant of the motion is the Hamiltonian (energy) or some multiple thereof. Hence, we can write the action J as
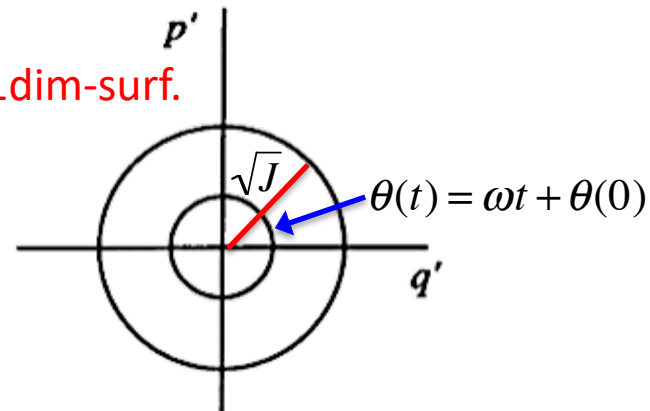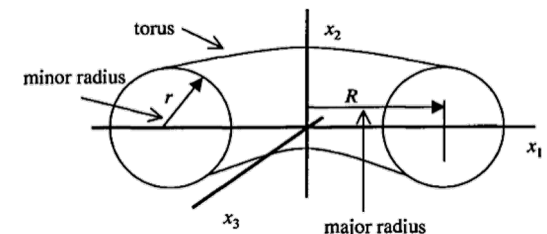
$$\boxed{H = \omega\ J} \longrightarrow J = \frac{H}{\omega} = \frac{p^2}{2m\omega} + \frac{kq^2}{2\omega} \qquad (8.4\text{-}10)$$

$$\omega = \frac{\partial H}{\partial J}$$
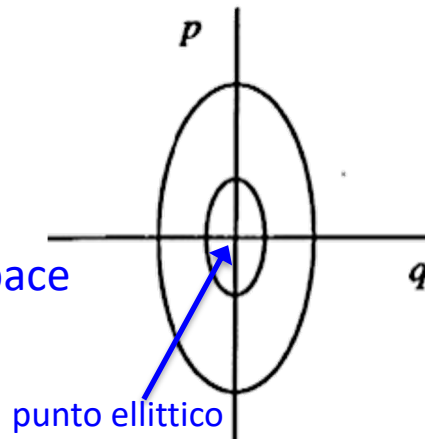
Toro: 1dim-surf.

$$\theta(t) = \omega t + \theta(0)$$
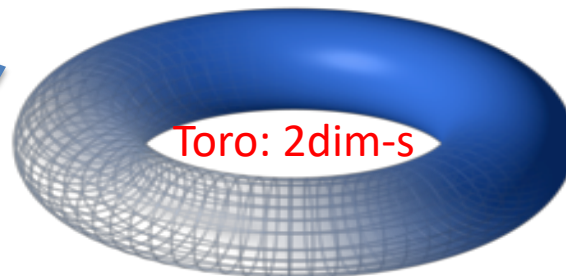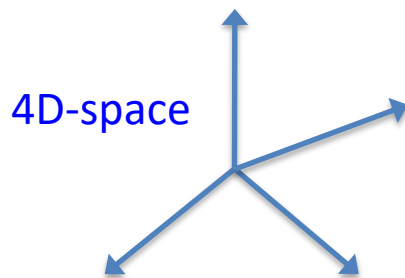
$\sqrt{J}$

2D-space

punto ellittico

Systems with N Degrees of Freedom

If we compare Eqs. (8.4-5) and (8.4-6) with the results of the simple harmonic oscillator example, we see that <u>an integrable system with N degrees of freedom is equivalent, in terms of action-angle variables, to a set of N uncoupled oscillators.</u> (The oscillators are simple harmonic if the ω_i are independent of the value of the Js. They are otherwise nonlinear oscillators for which ω depends on J.) This connection explains why so much attention is paid to oscillating systems in the study of dynamics.

2 gradi di libertà.   Since there are <u>N constants of the motion</u> for an integrable system of N degrees of freedom, the trajectories in state space are highly constrained. For example, an integrable <u>system with two degrees of freedom</u> has trajectories confined to a two-dimensional surface in phase space. This surface, in general, is the surface of a torus residing in the original four-dimensional phase space. Like the quasi-periodic motion studied in Chapter 6, the trajectories are characterized by the two frequencies

$$H = \omega_1 J_1 + \omega_2 J_2$$

$$\omega_1 = \frac{\partial H}{\partial J_1} \qquad \omega_2 = \frac{\partial H}{\partial J_2} \qquad \longrightarrow \qquad \frac{\omega_1}{\omega_2} \quad \text{winding number}$$

4D-space

Toro: 2dim-s

torus

minor radius

r

major radius

R

x_1

x_2

x_3

More generally, we say that a trajectory for an integrable system with *N* degrees of freedom is constrained to the *N*-dimensional surface of a torus (which resides in the original 2*N*-dimensional phase space). These tori are often called *invariant tori* since the motion is confined to these surfaces for all time.

If the various frequencies ω_i are incommensurate and the motion is quasi-periodic, then the trajectory eventually visits all parts of the torus surface. Such a system is said to be *ergodic* because one could compute the average value of any quantity for that system either by following the time behavior and averaging over time (usually hard to do) or by averaging over the *q, p* values on the surface of the torus in phase space (usually much easier to do).

N gradi di libertà

$$H = \omega_1 J_1 + \omega_2 J_2 + ... + \omega_N J_N$$

$$\omega_i = \dot{\theta}_i = \frac{\partial H}{\partial J_i} \qquad i = 1, ..., N$$
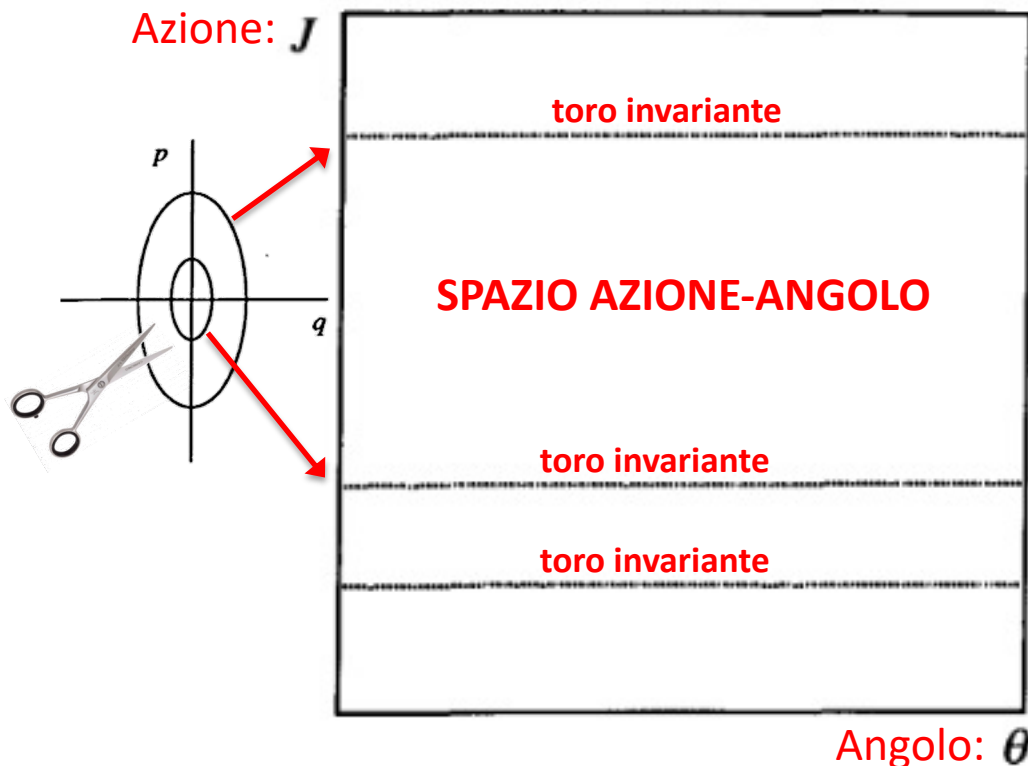
2N D-space

Toro: Ndim-s
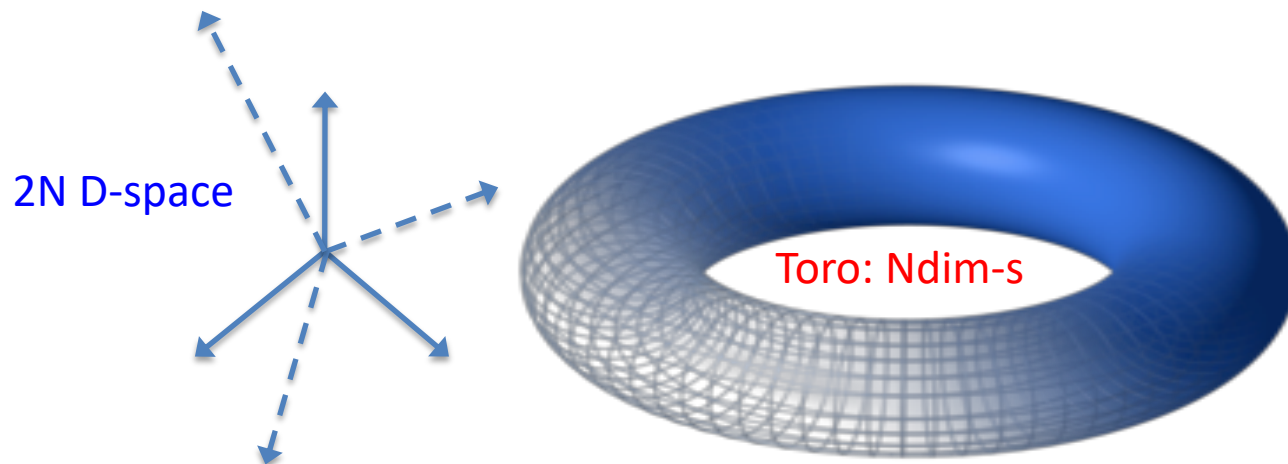
Ergodicity: time average = surface average

Action-Angle Space

Instead of the usual *pq* phase space, an alternative state space description makes use of the action-angle variables. The motivation for this is threefold. First, for an integrable system, each trajectory is characterized by a fixed value for each of the action variables. For example, for the simple harmonic oscillator, each elliptical trajectory in *pq* phase space corresponds to a fixed action as shown in Eq. (8.4-10).

In action-angle space, the trajectories of an integrable system reside on horizontal lines of constant action. Each horizontal line in Fig. 8.4 corresponds to a "torus" in the original *pq* phase space. (we may think of cutting the torus around its outer circumference and then spreading the "surface" flat. The horizontal line corresponds to viewing the surface edge on.)

Azione: J

p

q

toro invariante

SPAZIO AZIONE-ANGOLO

toro invariante

toro invariante

Angolo: θ

The second motivation for this kind of diagram comes from the study of nonintegrable systems. As we shall see in the next section, when a Hamiltonian system becomes nonintegrable, the action associated with a trajectory is no longer constant (in general). This fact shows up most obviously in an action-angle space diagram as the trajectory points wander vertically in that diagram.
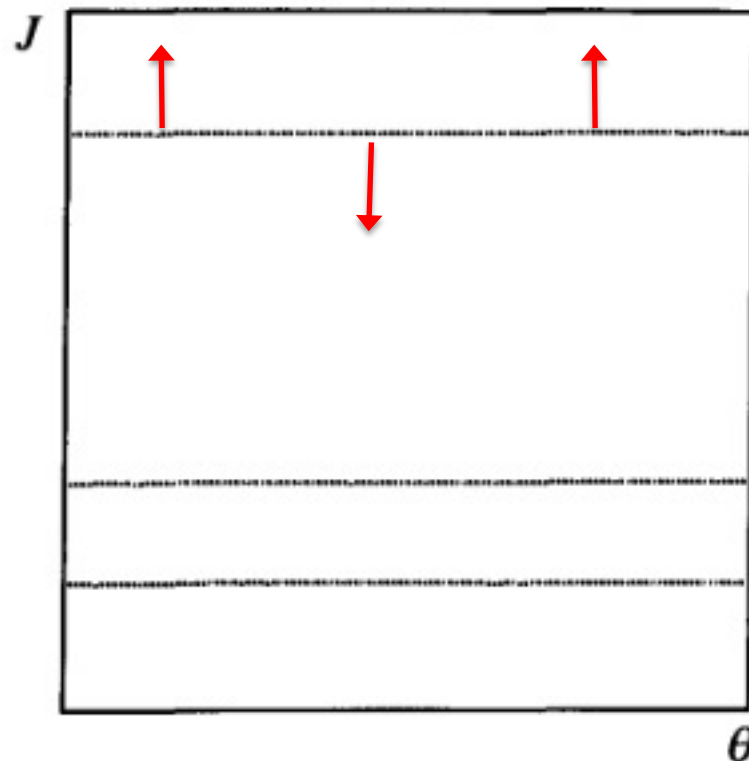
## 8.5 Nonintegrable Systems, the KAM Theorem, and Period-Doubling

Since the behavior of an integrable Hamiltonian system is always periodic or quasi-periodic, an integrable system cannot display chaotic behavior. We have spent some time describing integrable systems because much of the literature on the chaotic behavior of Hamiltonian systems has focused on systems that are, in some sense, just slightly nonintegrable. We can then ask how the behavior of the system deviates from that of an integrable system as the amount of nonintegrability increases.

We are immediately faced with the problem of visualizing the trajectories for nonintegrable systems because, as we learned in the last section, a nonintegrable system must have at least two degrees of freedom. If the system were integrable, then the trajectories would move on the two-dimensional surface of a torus and be either periodic or quasi-periodic. However, if the system is nonintegrable, then the trajectories can move on a three-dimensional surface in this four-dimensional phase space because the energy is conserved and hence still constrains the trajectories. This three-dimensional motion allows for the possibility of chaos.

Sistema Hamiltoniano ad almeno 2 gradi di libertà (almeno 2N=4 dimensioni): si può avere caos!

$$\begin{cases} \dot{q}_1 = \dot{x}_1 = f_1(x_1, x_2, x_3, x_4) \\ \dot{p}_1 = \dot{x}_2 = f_2(x_1, x_2, x_3, x_4) \\ \dot{q}_2 = \dot{x}_3 = f_3(x_1, x_2, x_3, x_4) \\ \dot{p}_2 = \dot{x}_4 = f_4(x_1, x_2, x_3, x_4) \end{cases}$$

Solo tre equazioni sono indipendenti perchè H è costante
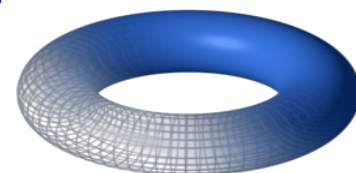
For an integrable two-degree-of-freedom system, we can think of the phase space as consisting of a set of nested tori (see Fig. 8.5). For fixed values of the two constants of the motion, the trajectories are confined to the surface of one of the tori. When the system becomes slightly nonintegrable, the trajectories begin to move off the tori, and we say that the tori are destroyed.

Poincaré sections are used to simplify the description further. We pick out a phase space plane that is intersected "transversely" by the trajectories and then record the points at which trajectories intersect that plane. For a two-degree-of-freedom system, we thereby reduce the description to a set of points in a two-dimensional plane.

Sistema Integrabile
$$H = \omega_1 J_1 + \omega_2 J_2$$

Sistema "leggermente" non Integrabile
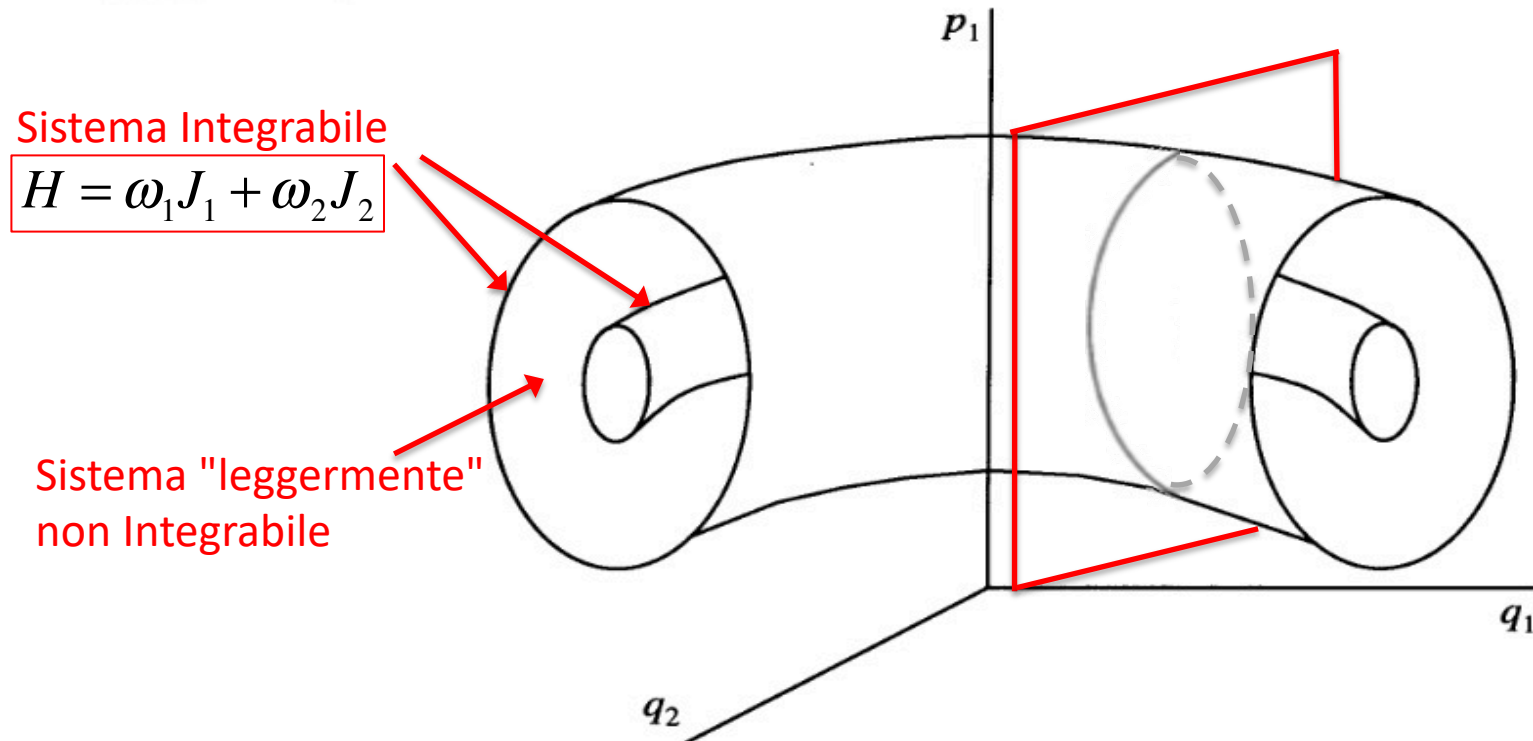
Fig. 8.5. For an integrable two-degree-of-freedom system, the trajectories are confined to the surfaces of a set of nested tori. Each surface corresponds to a different set of values of the two constants of the motion. If the system becomes nonintegrable, the trajectories can move off the tori.

For a general integrable two-degree-of-freedom system, the Poincaré plane will look like a (distorted) version of the phase space diagram for the pendulum: There will be *elliptic orbits*, which form closed paths around elliptic points. (As in Chapter 6, the paths will consist of a finite number of discrete points for periodic motion. For quasi-periodic motion, the intersection points fill in a continuous curve on the Poincaré plane.) In the neighborhood of hyperbolic points, there will also be *hyperbolic orbits*, some of which form apparent intersections at the hyperbolic (saddle) points. Figure 8.6 illustrates the Poincaré plane for the Hénon–Heiles system, discussed in more detail in Section 8.6.

Sistema integrabile 1 g.d.l.:
Pendolo
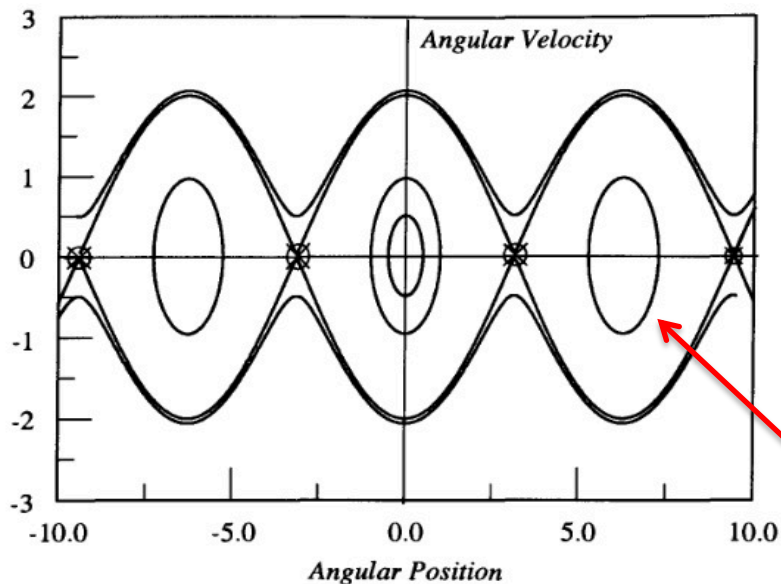
Sistema integrabile 2 g.d.l.:
ex. Hénon-Heiles

2dim Phase space

2dim Poincarè section

punti iperbolici

TORI

punti ellittici
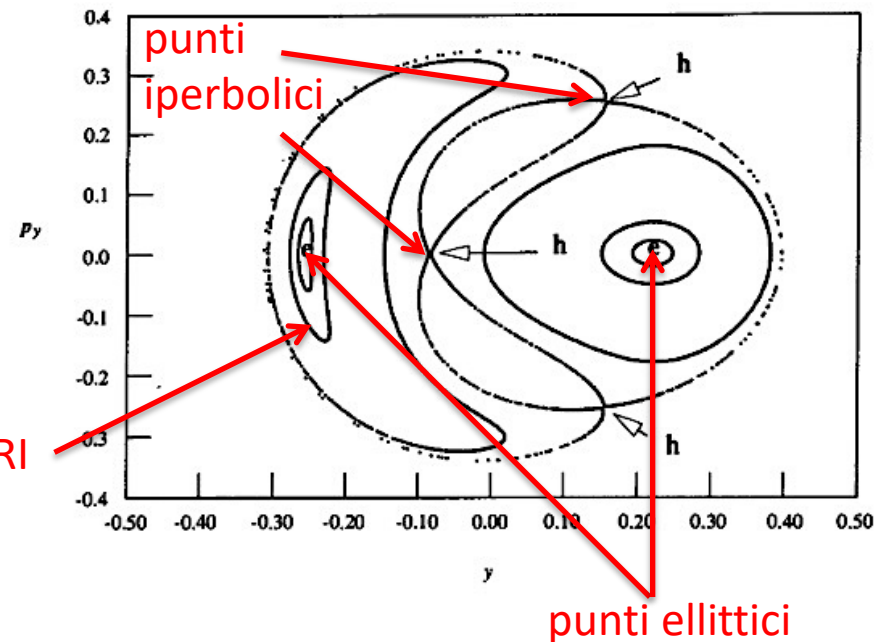
If the system becomes nonintegrable, constraints are removed from the trajectories, and they can begin to move more freely through phase space. Hence, loosely speaking, we expect the highly organized pattern of the integrable system's Poincaré section to "dissolve." Does the entire Poincaré section, however, dissolve simultaneously leaving only a random scattering of points? The answer to this question is provided by the famous ***Kolmogorov–Arnold–Moser (KAM) Theorem*** [Arnold, 1978].
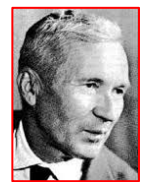
The KAM theorem states that (under various technical conditions that need not concern us here) some phase space tori, in particular those associated with quasi-periodic motion with an irrational winding number, survive (but may be slightly deformed) if a previously integrable system is made slightly nonintegrable. This result is stated more formally as follows: The originally integrable system's Hamiltonian can be written as a function of the action variables alone: $H_0(J)$. We now make the system nonintegrable by adding to $H_0(J)$ a second term, which renders the overall system nonintegrable. The full Hamiltonian is then

$$H(J,\theta) = H_o(J) + \varepsilon H_1(J,\theta) \qquad (8.5\text{-}1)$$

where ε is a parameter that controls the relative size of the nonintegrability term. The second term in (8.5-1) is sometimes called a "perturbation" of the original Hamiltonian, and "perturbation theory" is used to evaluate the effects of this term on the trajectories. The KAM Theorem states that for $\varepsilon \ll 1$ (so the system is almost integrable), the tori with irrational ratios of the frequencies associated with the actions will survive. These are called ***KAM tori***. As ε increases, the tori dissolve one by one with the last survivor being the one with winding number equal to our old friend the Golden Mean, the "most irrational" of the irrational numbers.

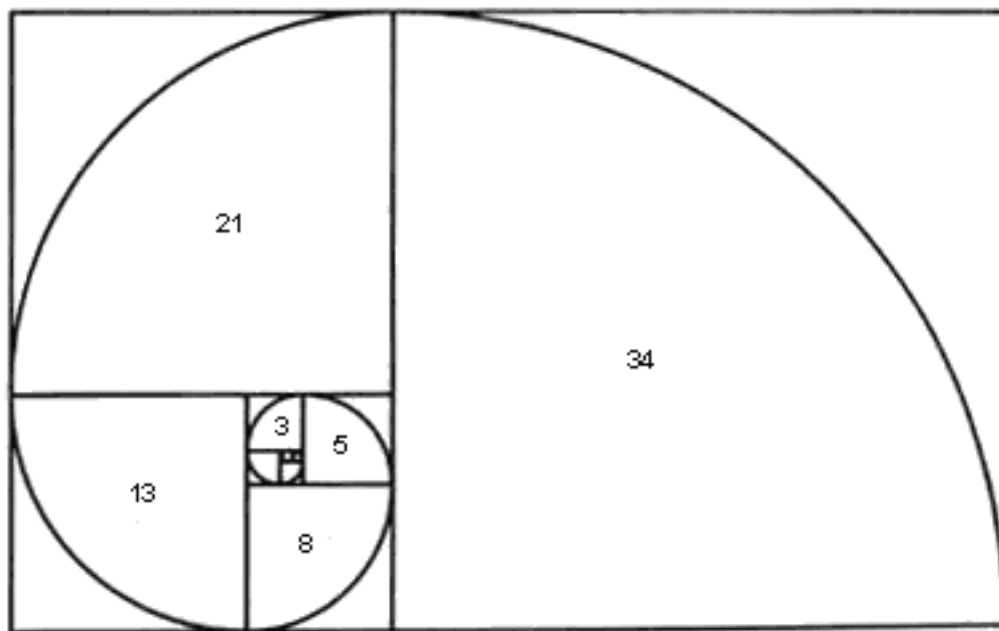winding number:

$$\frac{\omega_1}{\omega_2}$$

sezione aurea

$$\frac{a+b}{a} = \frac{a}{b} \equiv \varphi$$

$$\varphi = \frac{1+\sqrt{5}}{2} =$$
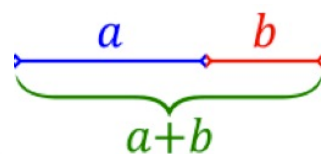
$$1.6180339887\ldots$$

golden ratio

Spirale Logaritmica

Successione di Fibonacci

1,1,2,3,5,8,13,21,34,55,89,144,233,377...

1/1   = 1
2/1   = 2
3/2   = 1.5
5/3   = 1.66666666666
8/5   = 1.6
13/8 = 1.625
21/13 = 1.61538461538
34/21 = 1.61904761905
55/34 = 1.61764705882
89/55 = 1.61818181818
—

1+1=2
1+2=3
2+3=5
3+5=8
5+8=13
8+13=21

Phi = 1.6180339887...

sezione aurea

$$\frac{a+b}{a} = \frac{a}{b} \equiv \varphi$$

$$\varphi = \frac{1+\sqrt{5}}{2} =$$
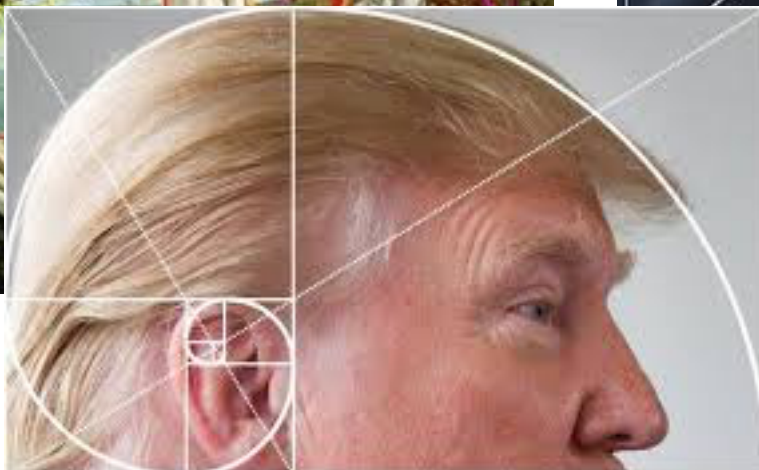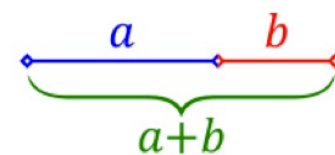
$$1.6180339887\ldots$$

golden ratio

As soon as ε increases above 0, the phase space tori associated with rational winding numbers break up. In a Poincaré section representation, the points begin to scatter around the Poincaré plane. This fast break-up can be explained as the kind of resonance effect discussed in Chapter 6. The nonintegrable part of the Hamiltonian essentially couples together what had been independent oscillations in the integrable case. When the frequency ratio for a torus is rational, there is considerable overlap of the harmonics associated with each oscillation. This overlap creates a "strong resonance" condition leading (usually) to a rapid growth of the amplitude of the motion in phase space and a rapid flight from the torus surface to which the trajectories had been confined in the integrable case. When the frequency ratio is irrational, however, there is no overlap in harmonics and we might expect the corresponding torus to survive for larger values of ε.

$$H(J,\theta) = H_o(J) + \varepsilon H_1(J,\theta)$$

2dim Poincarè section

irrational KAM tori

rational tori
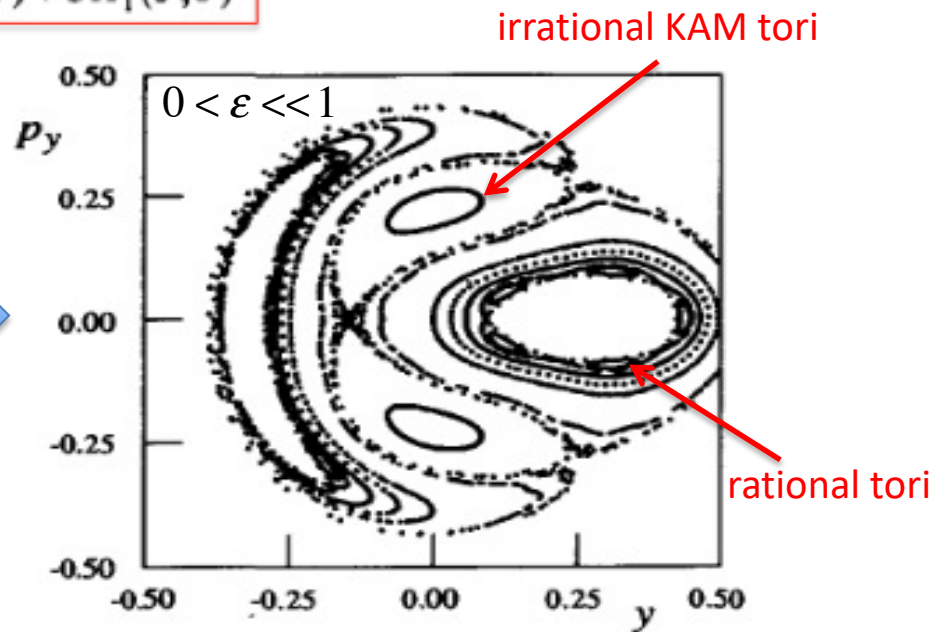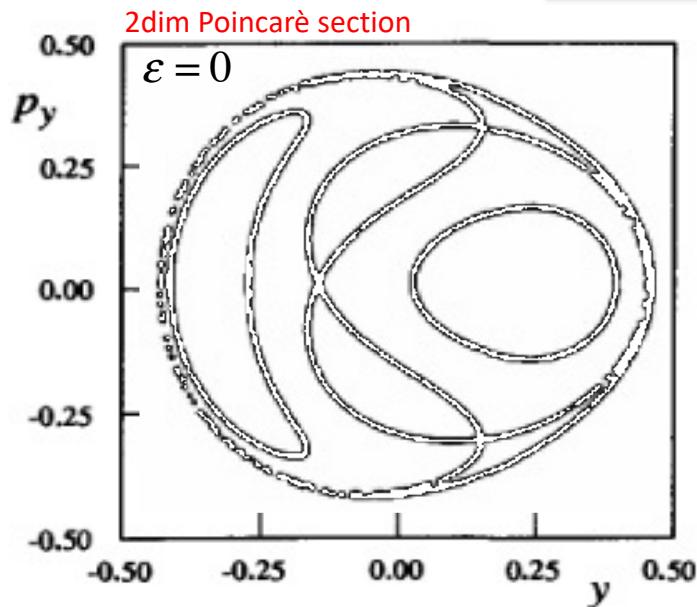
What is the dynamical importance of the KAM tori? In the integrable case, we argued that phase space trajectories are confined to the surfaces of tori in phase space. As the system becomes nonintegrable, trajectories are able to move off these tori. However, the surviving KAM tori still have trajectories associated with their surfaces. In low-dimensional phase spaces, the surviving KAM tori can prevent a trajectory that has moved off a dissolving torus from ranging throughout the allowed energy region of phase space. In a sense, the KAM tori continue to provide some organization for the trajectories in phase space.

$$H(J,\theta) = H_o(J) + \varepsilon H_1(J,\theta)$$

most irrational
KAM tori
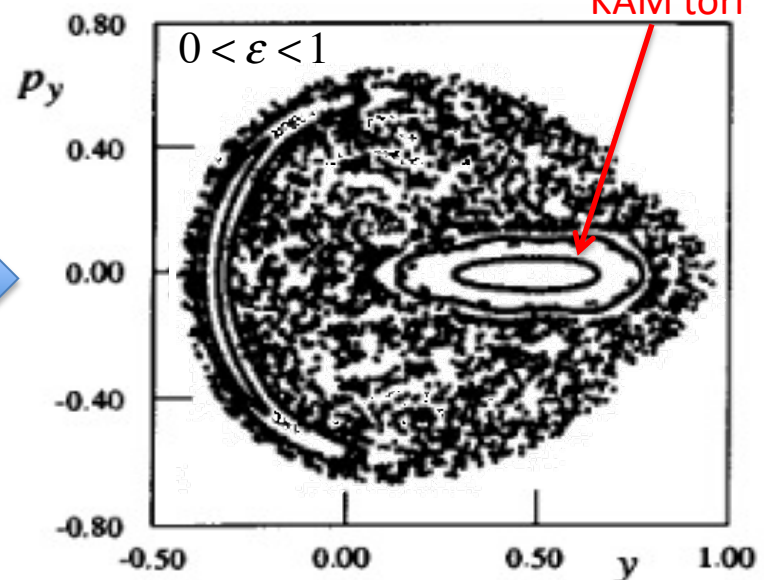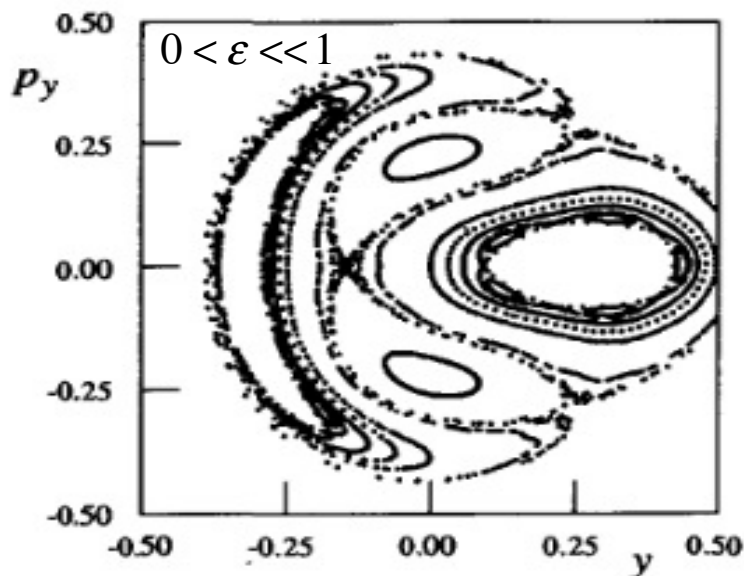
Let us see how this organizational ability depends on the dimensionality of the phase space (that is, on the number of degrees of freedom for the system). In a $2N$-dimensional phase space, the constant energy "surface" has $2N-1$ dimensions. As we argued earlier, the tori for an integrable system have a dimensionality of N. Thus, for the tori to partition phase space, we can have either $N=1$ or $N=2$. In other words, the tori can segregate regions of phase space only in systems with one or two degrees of freedom. In higher-dimensionality systems, when the tori begin to dissolve as the system becomes nonintegrable, a so-called **_stochastic web_** forms. In that case, trajectories may wander over large portions of the allowed energy region of state space. [Zaslevsky, Sagdeev, Usikov, and Chernikov, 1991] gives a very complete description of the formation of this stochastic web.
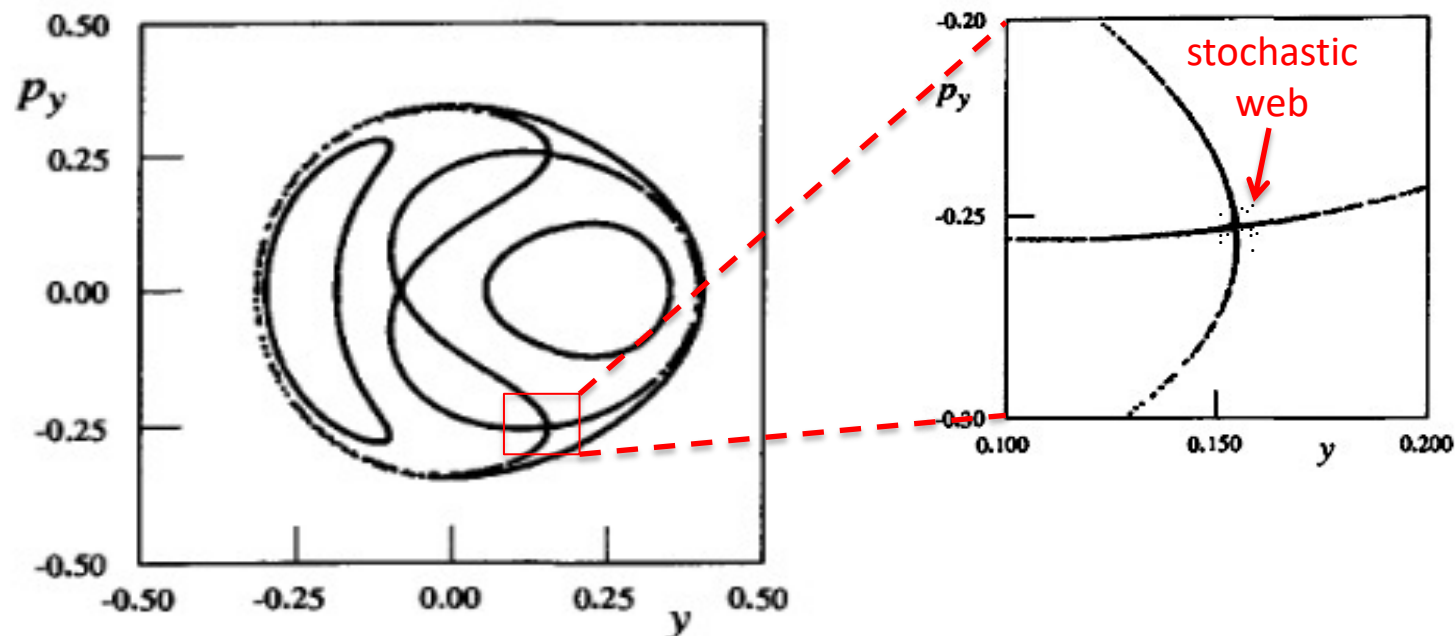
We can now appreciate one important difference between chaotic behavior in dissipative systems and chaos in Hamiltonian systems. In dissipative systems, initial conditions are not important because eventually the trajectories end up on an attractor. (Let us remind ourselves, however, that in general there may be several attractors for a given set of parameter values and different initial conditions may lead to trajectories ending up on different attractors.) However, in Hamiltonian systems, initial conditions are quite crucial. Some sets of initial conditions lead to regular behavior, while others lead to chaotic behavior. All of them have the same set of parameter values. As the amount of nonintegrability grows, however, the chaotic regions, in general, begin to crowd out the regular regions (or the regular regions, associated with the irrational winding number tori, shrink to allow the chaotic regions to grow).
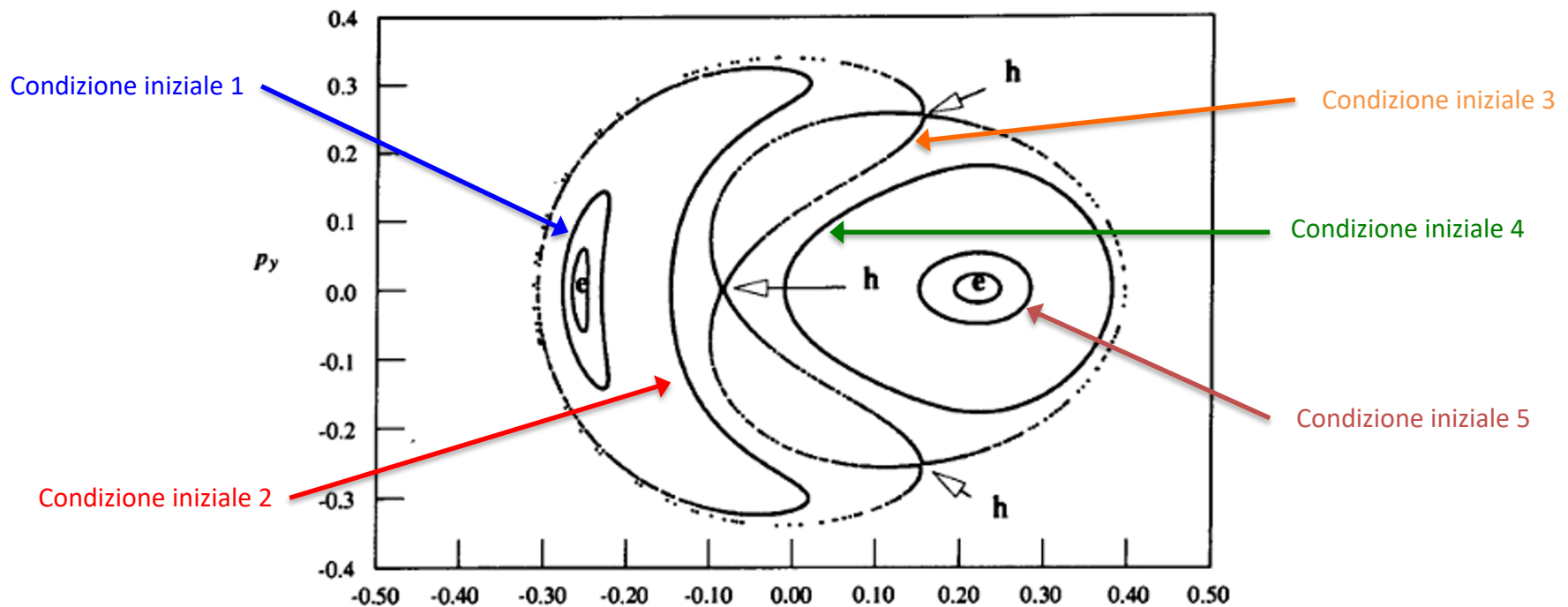
The Hénon-Heiles Hamiltonian

In this section we will explore the properties of a particular model Hamiltonian to illustrate the dynamics of Hamiltonian systems. The model was first introduced by Hénon and Heiles (HEH64) as a model for the motion of a star inside a galaxy. The Hamiltonian has two degrees of freedom (two pairs of ps and qs) and takes the form

$$H = \underbrace{\tfrac{1}{2}p_1^2 + \tfrac{1}{2}q_1^2 + \tfrac{1}{2}p_2^2 + \tfrac{1}{2}q_2^2}_{H_o(J)} + \underbrace{\left[q_1^2 q_2 - \tfrac{1}{3}q_2^3 \right]}_{\varepsilon H_1(J,\theta)} \qquad (8.6\text{-}1)$$

This Hamiltonian represents two simple harmonic oscillators (compare Exercise 8.2-2) coupled by a cubic term, which makes the Hamiltonian nonintegrable. If we let $q_1 = x$, $q_2 = y$, $p_1 = p_x$, and $p_2 = p_y$, then the Hamiltonian can also be interpreted as a model for a single particle moving in two dimensions under the action of a force described by a potential energy function

$$V(x, y) = \tfrac{1}{2}x^2 + \tfrac{1}{2}y^2 + x^2 y - \tfrac{1}{3}y^3 \qquad (8.6\text{-}2)$$

This potential energy function has a local minimum at the origin ($x = 0$, $y = 0$).

V(0,0)

V(x,y)

Michel Hénon
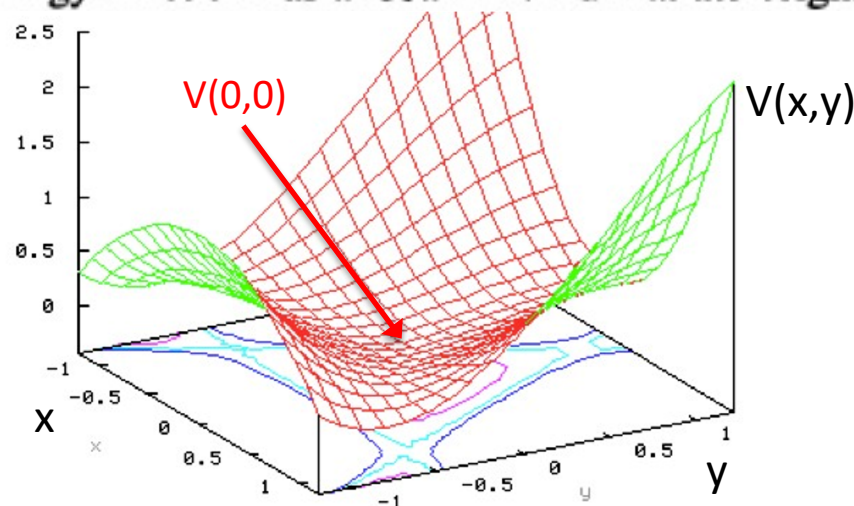
Carl Eugene Heiles

A three-dimensional plot of this potential energy function is shown on the left in Fig. 8.8. A contour plot of the same potential energy function is shown on the right of Fig. 8.8.
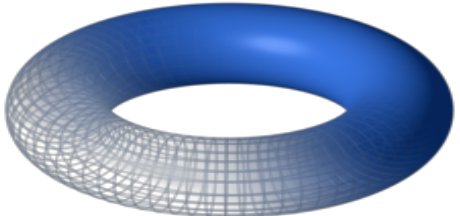
E<0.16666...

If we start the particle near the origin with an energy value less than 1/6, it will stay in an "orbit" near the origin for all time. If the energy is greater than 1/6, the particle can escape the local minimum of the potential energy and go off to infinity. If the energy is very small, the particle stays close to the origin and the trajectories look much like the periodic motion of a particle in a two-dimensional simple harmonic potential.

E<1/6
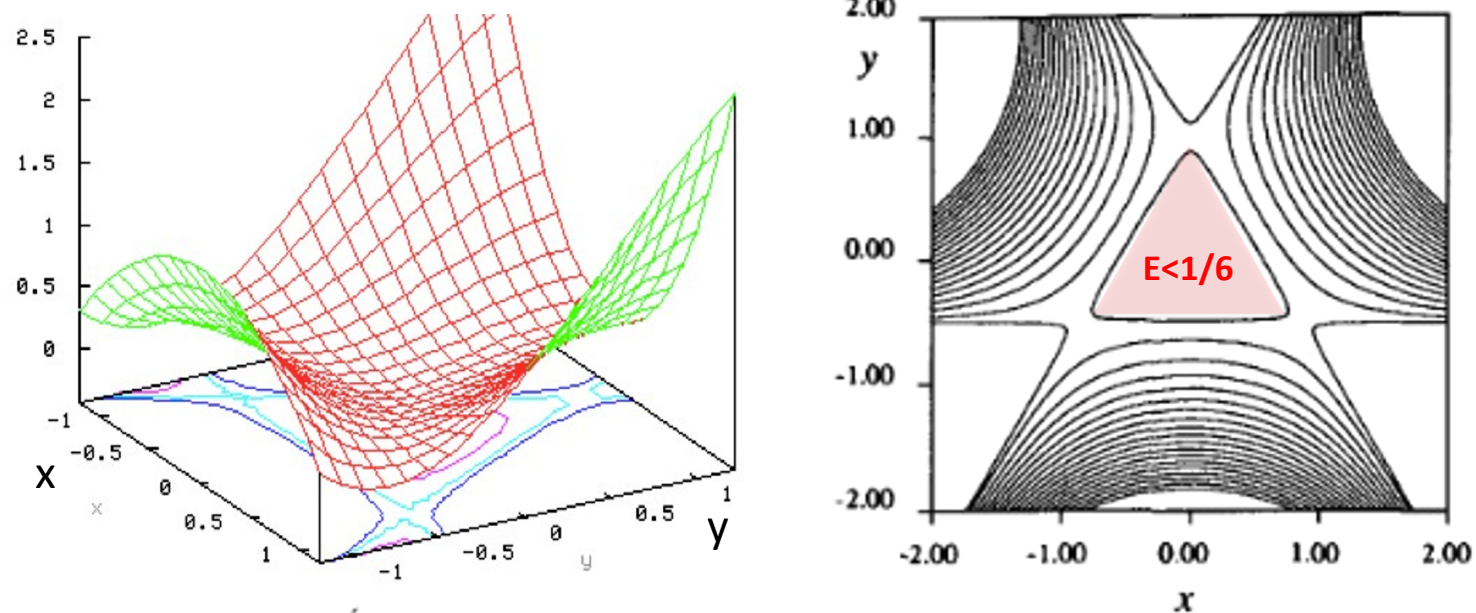
Fig. 8.8. On the left is a three-dimensional plot of the potential energy function for the Hénon–Heiles model. On the right is a contour plot of the same function. We will be concerned with a particle moving in the slight depression near the origin. If the particle's energy is less than 1/6, the particle will be trapped in the triangular region near the origin. For higher energies the particle can escape the local minimum of the potential energy.

Hamilton's equations for this system lead to the following equations for the dynamics of the system:

$$H = \frac{1}{2}p_x^2 + \frac{1}{2}p_y^2 + \frac{1}{2}x^2 + \frac{1}{2}y^2 + x^2y - \frac{1}{3}y^3$$

$$\begin{cases} \dot{x} = \dfrac{\partial H}{\partial p_x} = p_x \\[2mm] \dot{y} = \dfrac{\partial H}{\partial p_y} = p_y \\[2mm] \dot{p}_x = -\dfrac{\partial H}{\partial x} = -x - 2xy \\[2mm] \dot{p}_y = -\dfrac{\partial H}{\partial y} = -y - x^2 + y^2 \end{cases} \tag{8.6-3}$$

We see that the system lives in a four-dimensional phase space. However, since the system is Hamiltonian, the energy conservation constraint means that the trajectories must live in a three-dimensional volume in this four-dimensional space. Again, we will use the Poincaré section technique to reduce the recorded trajectory points to a two-dimensional plane.

Exercise 8.6-1. Verify that Hamilton's equations lead to the results shown in Eq. (8.6-3). Verify explicitly that Eqs. (8.6-3) lead to no volume contraction in phase space.

Let us examine in some detail how a Poincaré section of the phase space motion of the particle can be understood. It is traditional to plot the trajectory location on the yp_y plane when $x = 0$. We shall follow that tradition. In generating the Poincaré section, we first pick an energy value E and then some initial point on the Poincaré plane consistent with that energy value. For $x = 0$, the y and p_y values must satisfy

$$E = \tfrac{1}{2}p_x^2 + \tfrac{1}{2}p_y^2 + \tfrac{1}{2}y^2 - \tfrac{1}{3}y^3 \qquad (8.6\text{-}4)$$

Hence, for a fixed energy and a particular initial value for p_x, there is a finite range on the $y\,p_y$ plane within which the Poincaré section points must fall. The time evolution equations (8.6-3) are then integrated and successive Poincaré section points are generated.

condizioni iniziali x=0.5 y=0.5 px=0.5 py=0.9
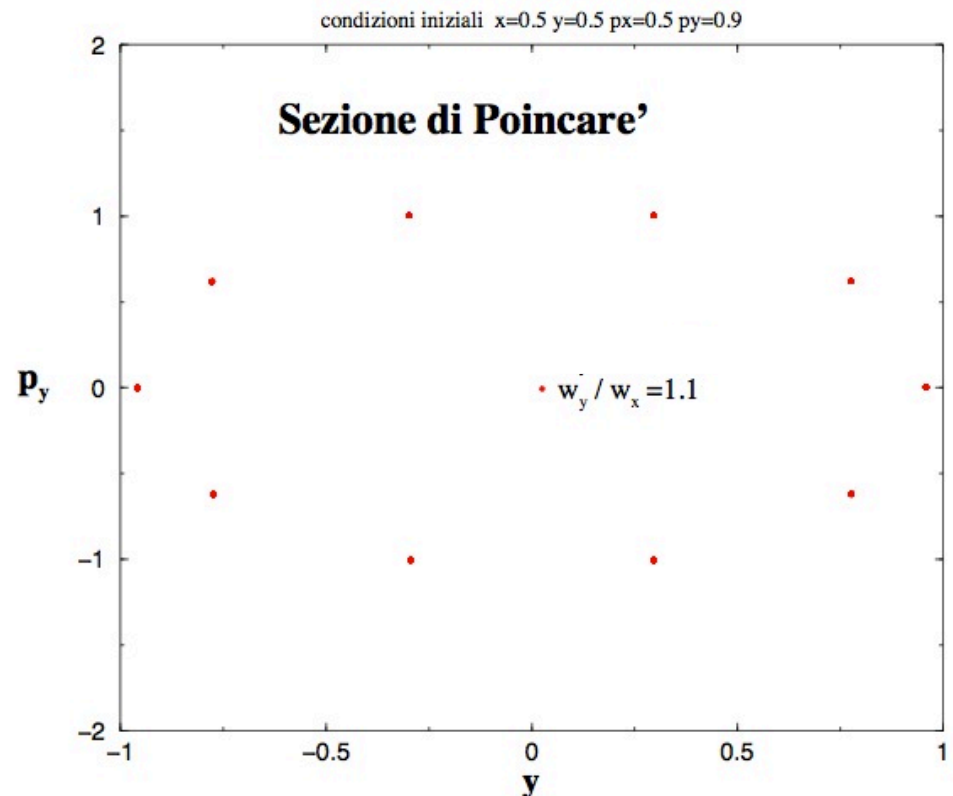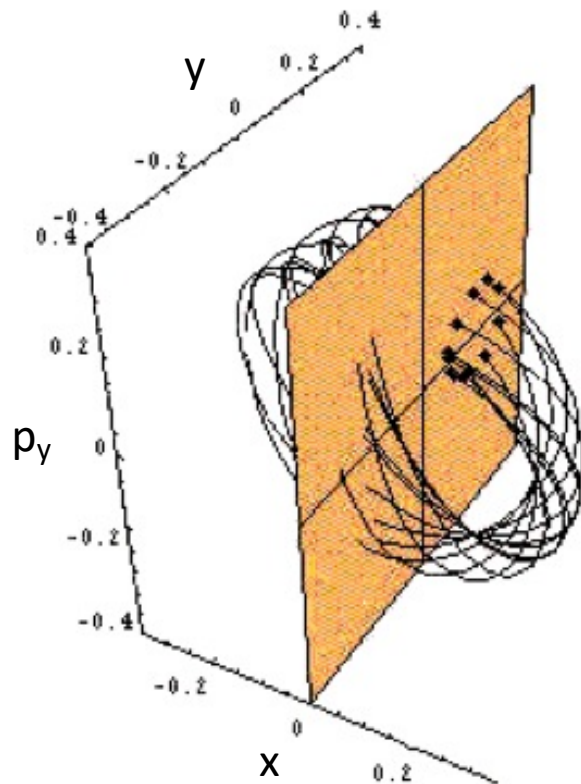
Sezione di Poincare'

$w_y / w_x = 1.1$

Figure 8.9 shows one such orbit in the xy (real space) plane on the left. On the right is the corresponding Poincaré section. The Poincaré section points fall on two "ellipses" that are formed by the intersection of a surface of a three-dimensional torus with the Poincaré plane. (Note that the cross section of the torus is distorted and the part of the torus intersecting the plane for negative values of y has a shape different from the part intersecting at positive values of y.) Thus, we conclude that this particular orbit corresponds to a periodic or quasi-periodic orbit. Near the middle of each of the ellipses is an elliptic point, not shown in Fig. 8.9.
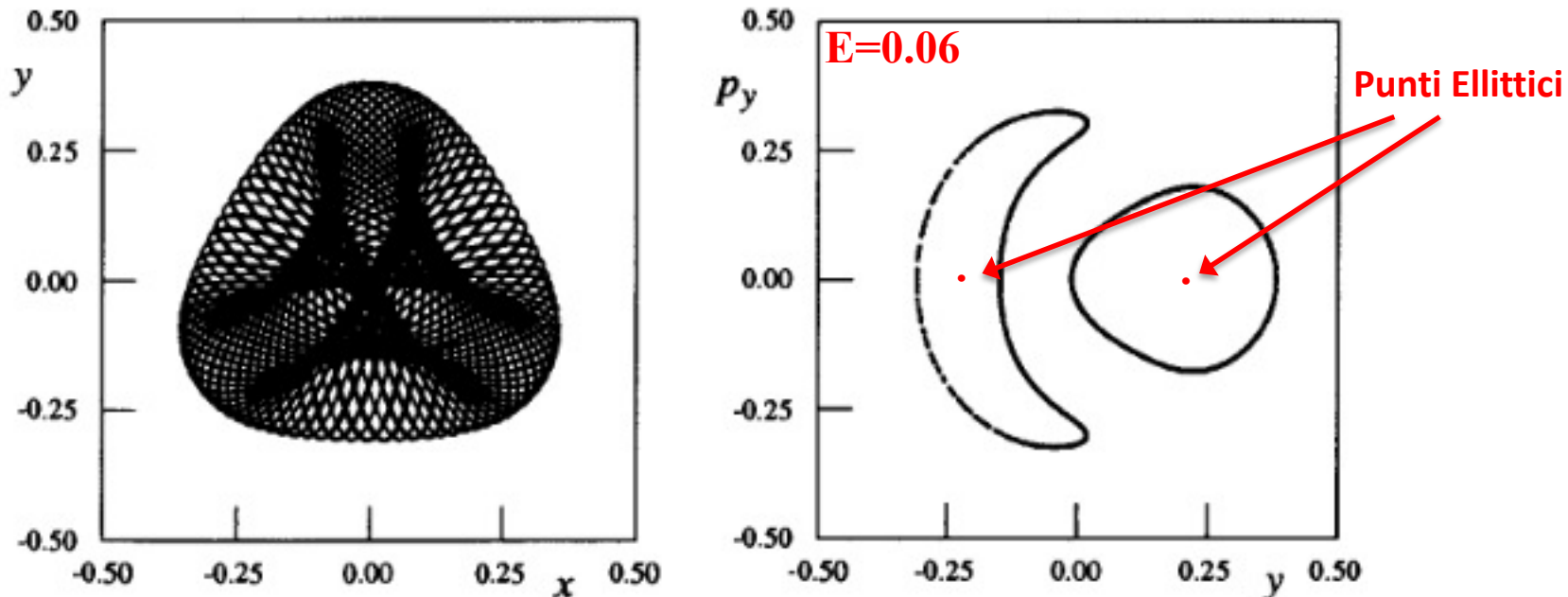
Fig. 8.9. On the left is the xy (real space) trajectory of a particle moving in the Hénon–Heiles potential with $E = 0.06$. The orbit started with $x = 0$, $y = -0.1475$, $p_x = 0.3101$, and $p_y = 0$. On the right is the corresponding p_y–y Poincaré section with $x = 0$. The "ellipses" are formed by the intersection of the surface of a three–dimensional torus with the Poincaré plane.

Note that the trajectory shown in Fig. 8.9 is just one of many trajectories possible for the given energy value. To fill out the Poincaré section, we need to choose a variety of initial conditions consistent with the same energy value. Figure 8.10 shows another orbit (in the xy plane) and its corresponding Poincaré section for the same energy value used in Fig. 8.9. This orbit approaches and is then repelled by three hyperbolic points located near the regions of apparent intersection. Near those hyperbolic points, the trajectory points are smeared and indicate (tentatively) that the behavior is chaotic. However, the chaotic behavior is confined to very small regions of the Poincaré plane. Thus, we see that chaotic orbits and quasi-periodic orbits coexist for the same energy value for Hamiltonian systems. Some initial conditions lead to chaotic orbits, while some lead to quasi-periodic orbits.
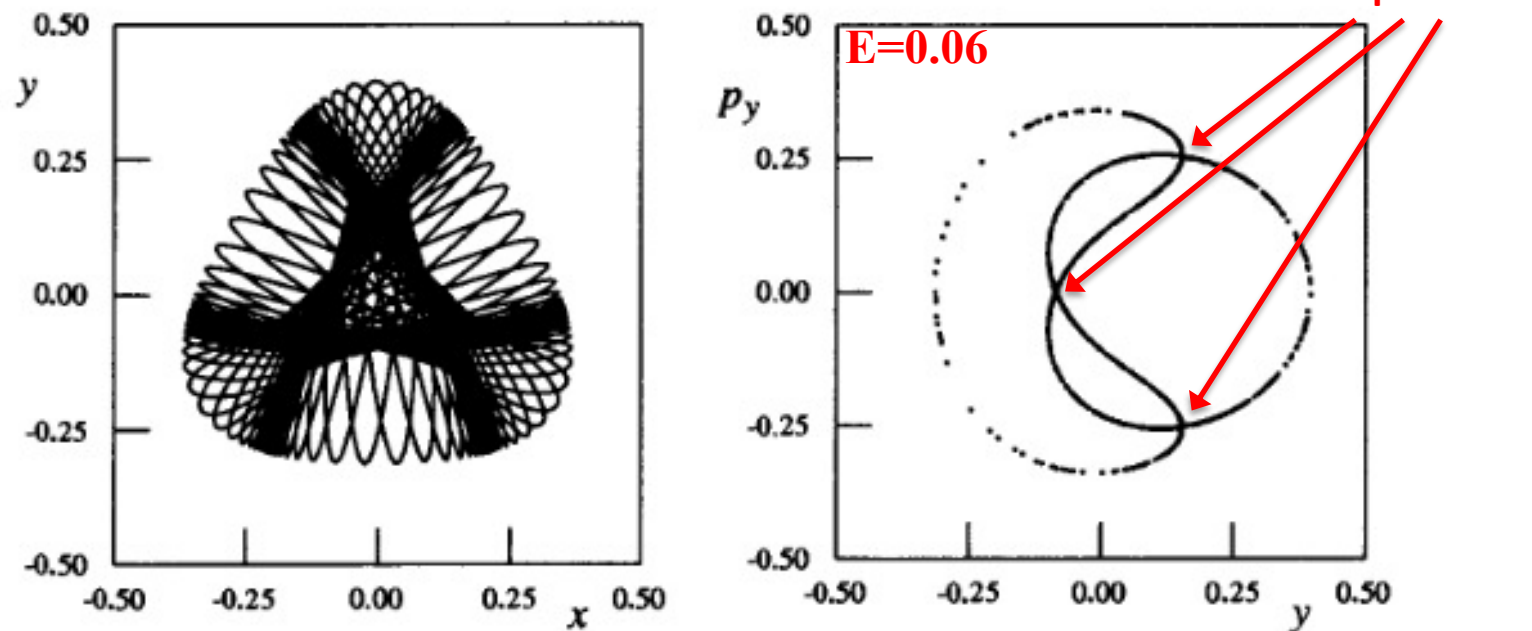
Fig. 8.10. On the left is another orbit of the Hénon–Heiles potential for $E = 0.06$, but with initial conditions different from those in Fig. 8.9. On the right is the corresponding $y\, p_y$ Poincaré section.
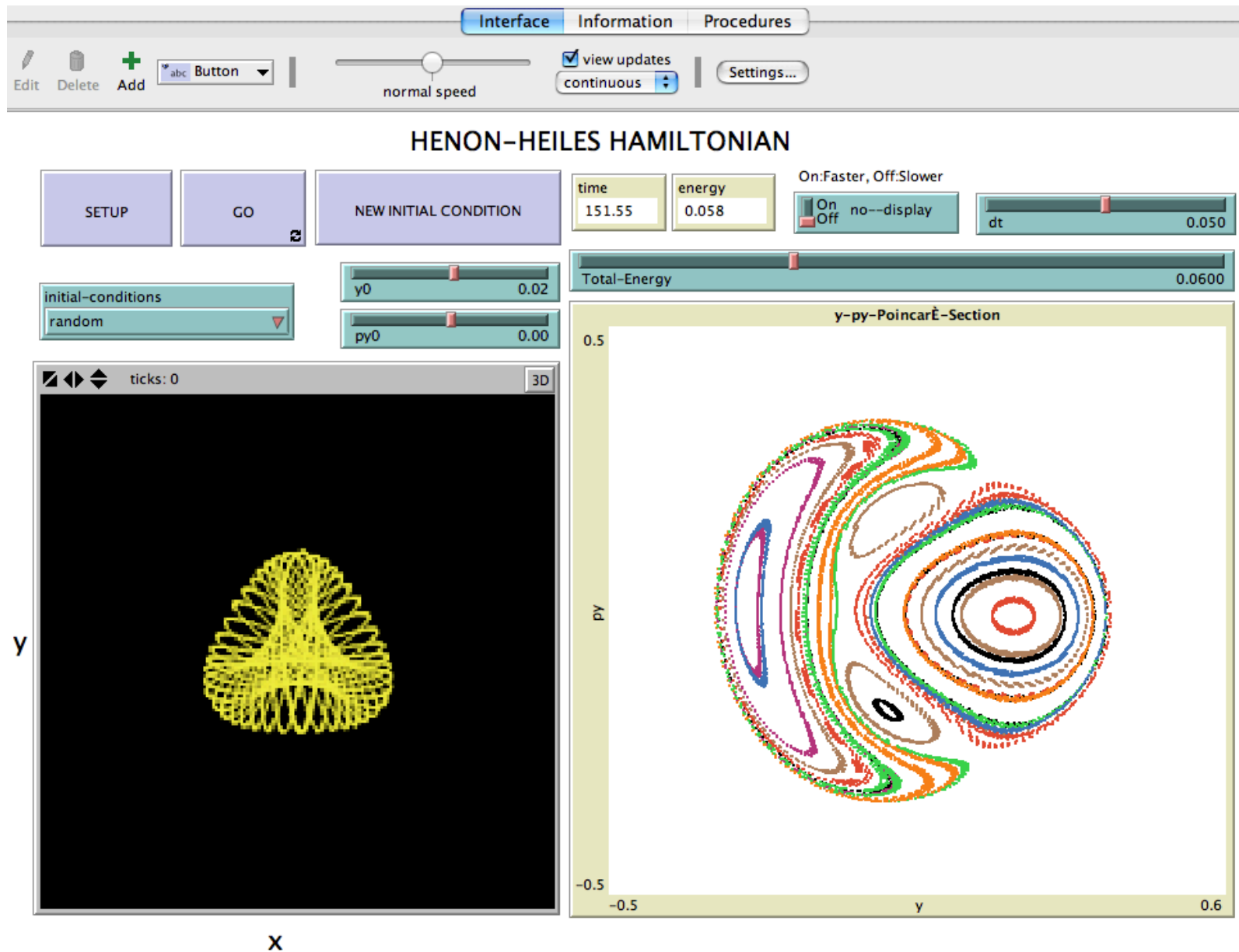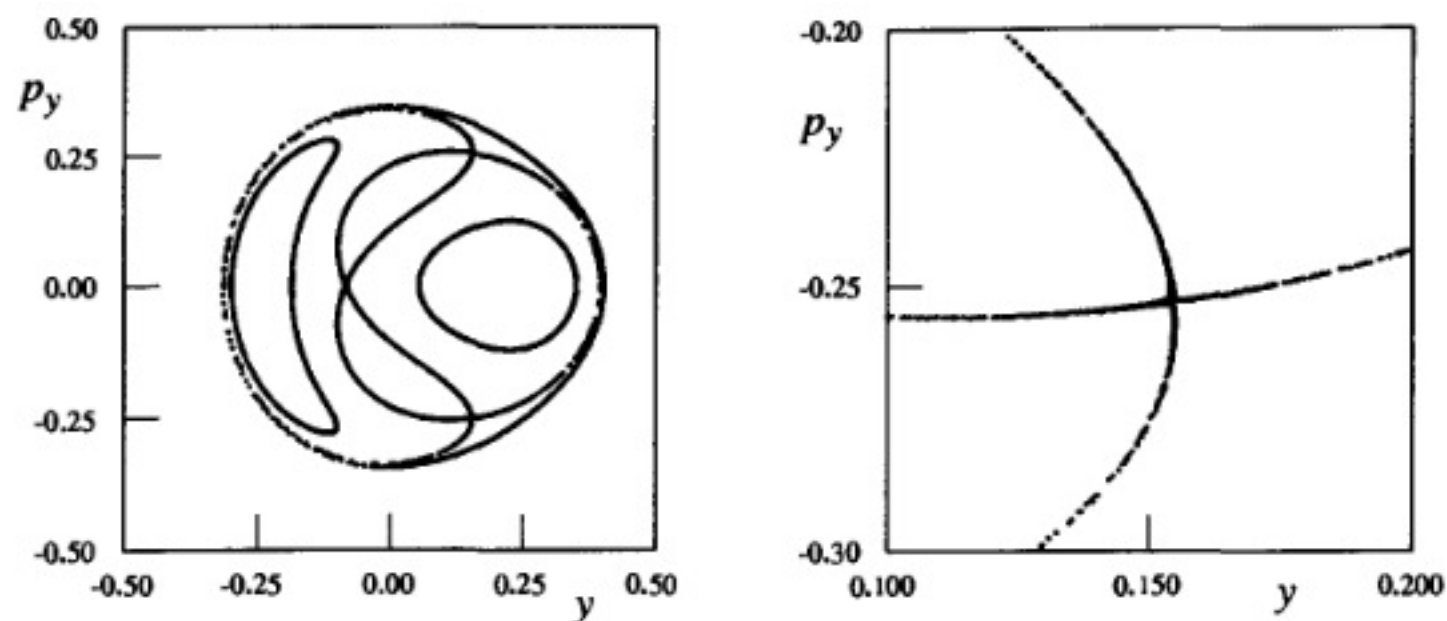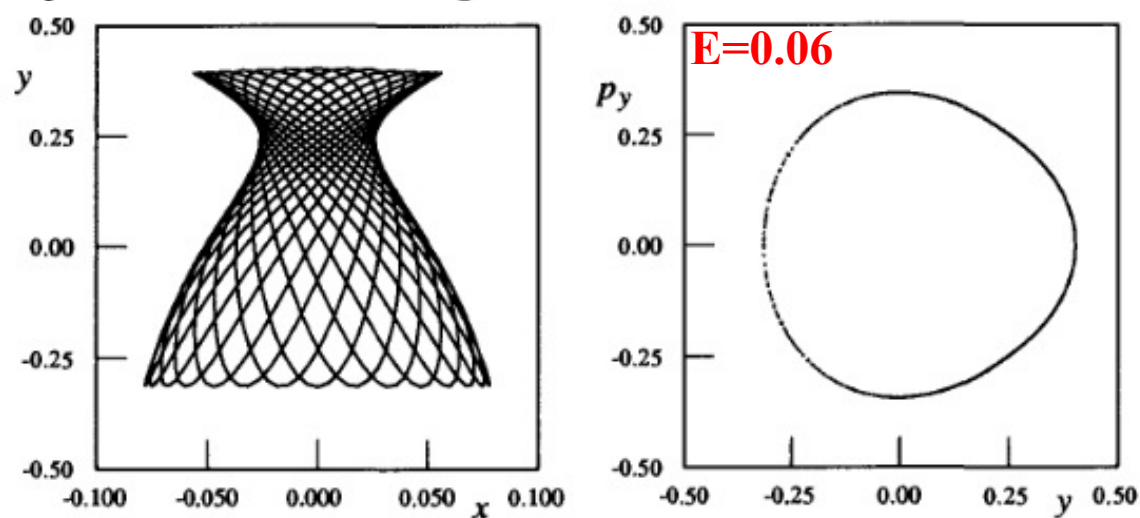
henon-heiles.nlogo

Figure 8.11 shows a more complete Poincaré section with several initial conditions used to generate a variety of trajectories, all with $E = 0.06$. Note that there is an outer boundary for the allowed intersection points in the yp_y plane (with $x = 0$). Points outside this boundary correspond to trajectories associated with energy values different from $E = 0.06$. The right-hand side of Fig. 8.11 shows a magnified view of the region near the lower hyperbolic point. The chaotic behavior of the intersection points is more obvious. The chaotic regions associated with these hyperbolic points are sometimes called *stochastic layers* or *stochastic webs*. These layers are due to homoclinic and heteroclinic tangles that develop from the stable and unstable manifolds associated with the hyperbolic (saddle) points.

Fig. 8.11. On the left is an $x = 0$, yp_y Poincaré section for the Hénon–Heiles system with $E = 0.06$. On the right is a magnified view of one of the regions near a hyperbolic point. The (slight) smear of intersection points is a symptom of a chaotic orbit.

The orbits that come close to the hyperbolic points are close to the separatrices associated with those points. For most Hamiltonian systems, those separatrices segregate regions of qualitatively different behavior. In the Hénon–Heiles system, trajectories associated with Poincaré section "curves" that lie outside the separatrices correspond to motion that lies close to the y axis for the real space trajectories. Figure 8.12 shows the trajectory associated with the Poincaré section curve that bounds the allowed region. The vase-shaped real space trajectory is qualitatively different from the trajectories associated with the inner ellipses in the Poincaré section (shown in Figs. 8.9 and 8.10). Since the orbits close to the separatrices are on the border between the two types of behavior, they are **quite** sensitive to perturbations, and they are the first to show signs of chaotic behavior when the system becomes nonintegrable.

E=0.06

Fig. 8.12. On the left is the xy (real space) trajectory of the Hénon–Heiles model with $E = 0.06$ and an initial point chosen to generate the Poincaré section shown on the right with intersection points that lie on the outer boundary of the allowed energy region. Since this Poincaré section curve is outside the separatrices associated with the hyperbolic points (see Fig. 8.10), the xy trajectory is qualitatively different from the trajectory (shown in Fig. 8.9) for Poincaré curves inside the separatrices.

Let us now increase the energy of the particle and see how the Poincaré section changes. For larger values of the energy, we expect the particle to roam over a wider range of xy values and hence the cubic potential term that causes the nonintegrability should become more important.

In Fig. 8.13, we have plotted the yp_y Poincaré section (again with $x = 0$) for $E = 0.10$. The Poincaré section has the same general structure seen in Fig. 8.11: There are two clusters of ellipses around the two elliptic points and an intertwining trajectory that gets near the three hyperbolic points; however, here the orbit associated with the hyperbolic points is more obviously chaotic. In fact, the entire chaotic set of points was generated from a single trajectory launched near one of the hyperbolic points.
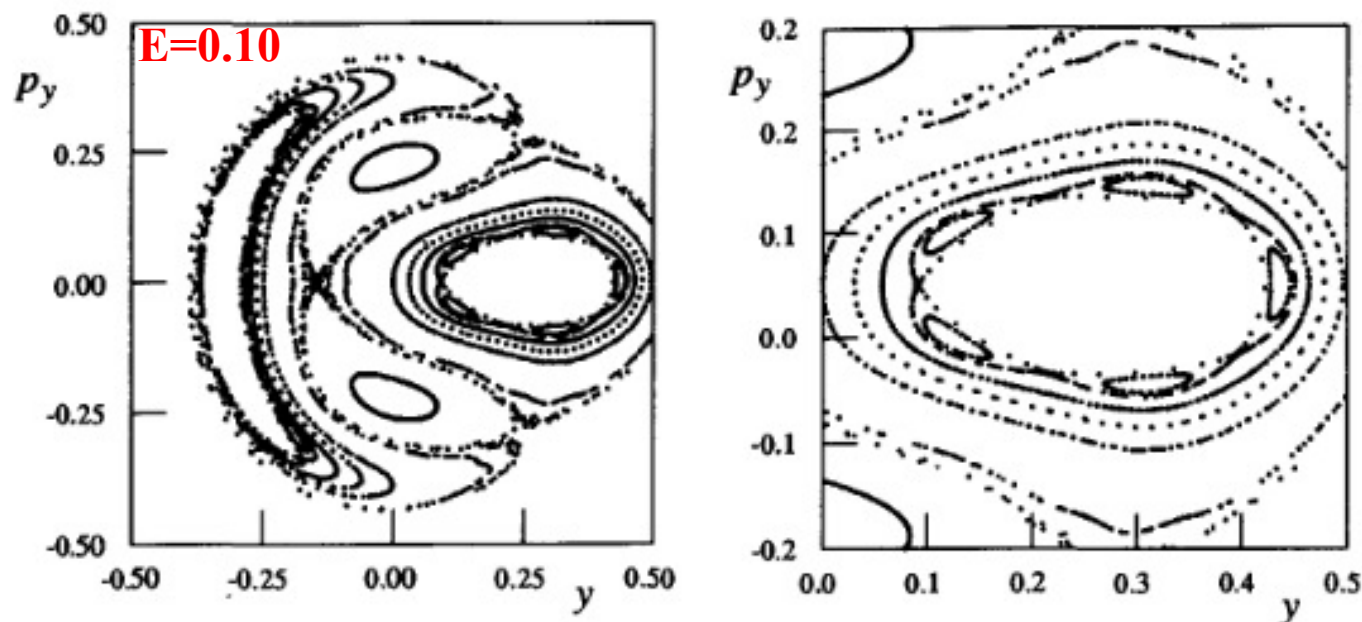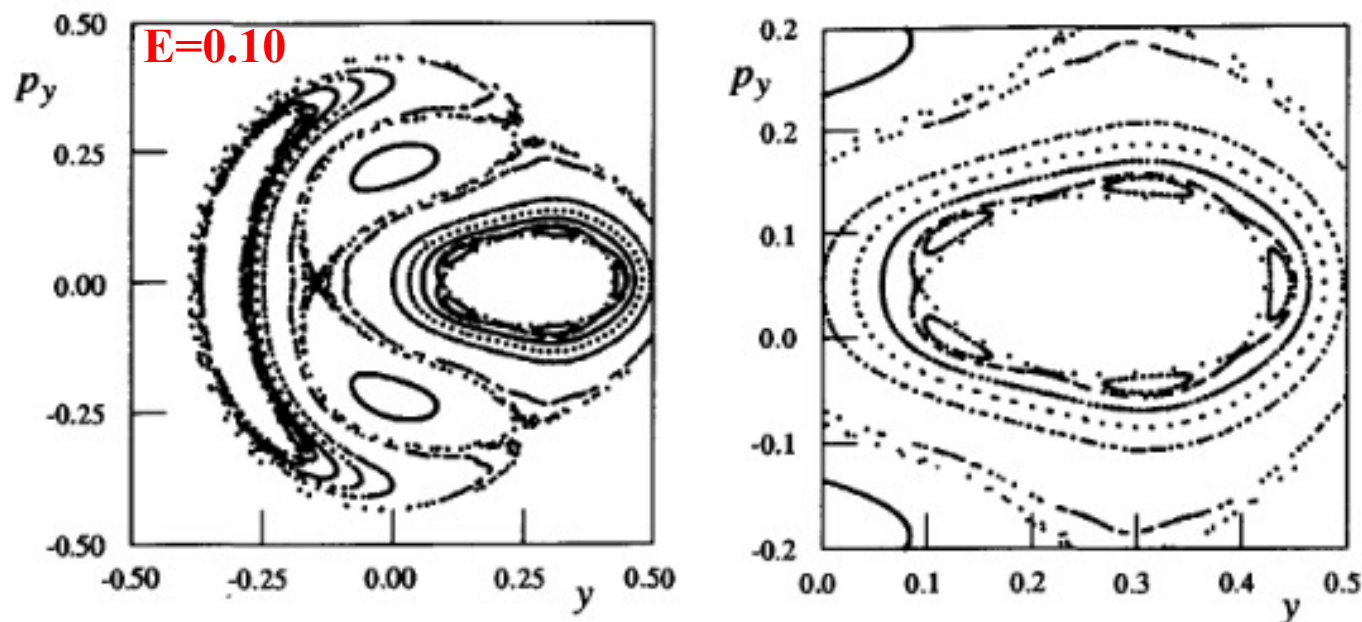

Fig. 8.13. On the left is the Poincaré section for the Hénon–Heiles model with $E = 0.10$. On the right is a magnified view of one of the archipelago island chains of elliptic and hyperbolic points that form from a KAM torus. Surrounding this chain are other surviving KAM tori.

A new feature, however, appears as well. On the left in Fig. 8.13, an elliptical band around each of the elliptic points seems to be smeared. On the right of Fig. 8.13, a magnified view of one of these bands shows that the band is actually a cluster (an "archipelago") of five elliptical curves interlaced with an orbit that gets near to five hyperbolic points. You should note that the five elliptical curves were generated by a <u>single</u> trajectory; therefore, these curves should be thought of as cross sections of a "snake" tube that wraps around the main "inner" elliptical tube five times. Similarly, the "necklace" associated with the hyperbolic points is the trace of a single trajectory.
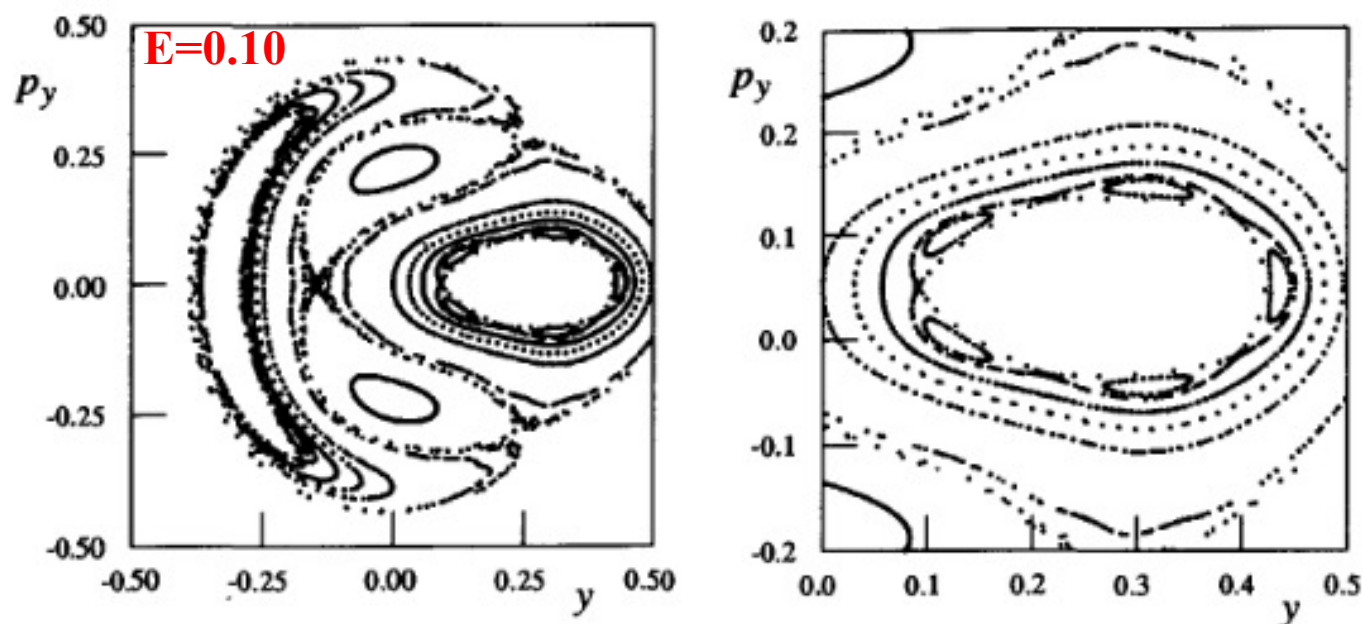
Fig. 8.13. On the left is the Poincaré section for the Hénon–Heiles model with $E = 0.10$. On the right is a magnified view of one of the archipelago island chains of elliptic and hyperbolic points that form from a KAM torus. Surrounding this chain are other surviving KAM tori.

As the energy of the system has increased, the nonintegrable part of the Hamiltonian becomes more important, and the KAM tori corresponding to irrational winding numbers begin to dissolve. Each one dissolves by breaking up into a series of elliptical islands interlaced with a (chaotic) trajectory associated with the hyperbolic points that are "born" when the islands form.

The chaotic trajectory associated with one archipelago, however, is not connected to the chaotic trajectories associated with other clusters of hyperbolic points. In a sense, the remaining KAM tori act as barriers and keep the chaotic trajectories, which would like to roam throughout phase space, confined to certain regions. (Again, we should remind ourselves that this is a feature unique to systems with two degrees of freedom.)
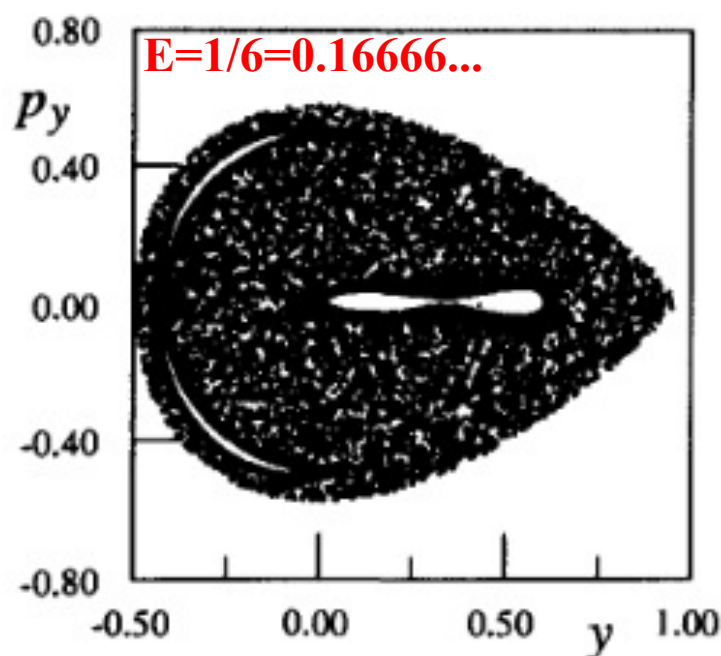

Fig. 8.13. On the left is the Poincaré section for the Hénon–Heiles model with $E = 0.10$. On the right is a magnified view of one of the archipelago island chains of elliptic and hyperbolic points that form from a KAM torus. Surrounding this chain are other surviving KAM tori.

However, if the energy is increased further, the KAM tori continue to dissolve and a single chaotic trajectory eventually wanders throughout almost the entire allowed region of the Poincaré section (consistent with the conservation of energy). Figure 8.14 shows Poincaré sections with $E = 0.14$ (on the left) and $E = 0.16$ (on the right). The scattered dots were all produced from one trajectory that now wanders considerably through the phase space. Some vestiges of KAM tori can still be seen, but they occupy a considerably smaller region of phase space.
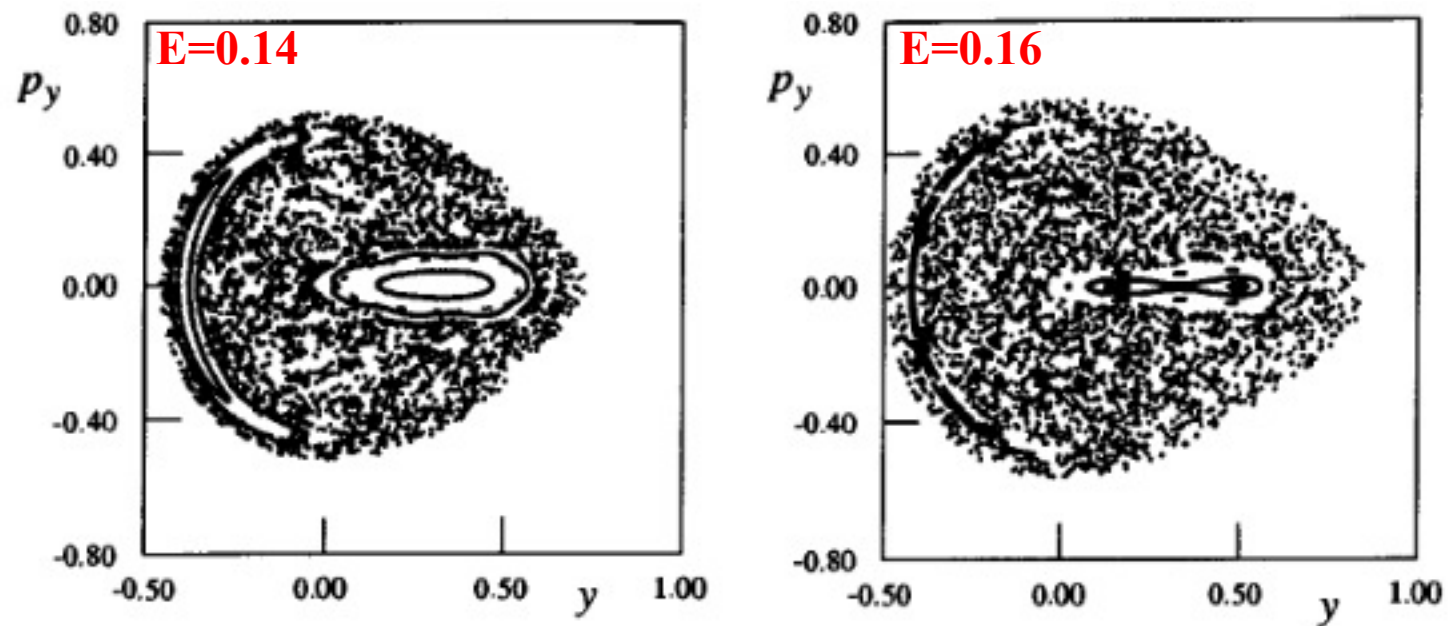
Fig. 8.14. On the left is the Poincaré section (for $x = 0$) yp_y plane for the Hénon–Heiles model with $E = 0.14$. On the right we have $E = 0.16$. In both cases the scattered points were all produced by launching a single trajectory that wanders chaotically through the allowed region of phase space.
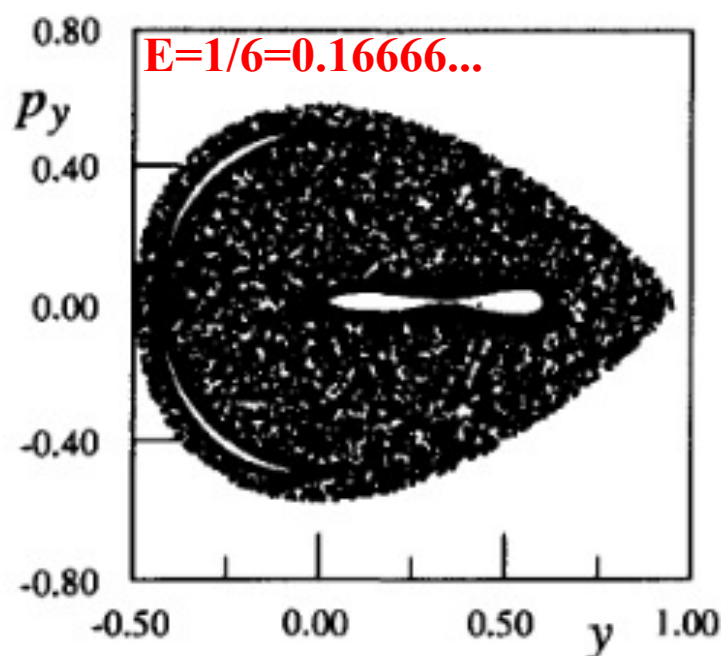
Let us summarize what we have seen with the Hénon–Heiles model. For low values of the energy, most of the trajectories are associated with quasi-periodic trajectories (KAM tori). Chaotic behavior is present, but it is barely noticeable because it is confined to very small regions of phase space. As the energy increases, the KAM tori begin to dissolve via archipelago formation. The chaotic regions begin to expand. However, for a two-degree-of-freedom system, the remaining KAM tori prevent a given chaotic trajectory from wandering over the entire allowed region of phase space. After the last KAM torus (associated with the Golden Mean winding number) has disappeared, a single chaotic trajectory covers almost the entire allowed region of phase space as shown in Fig. 8.15.

Fig. 8.15. A Poincaré section $(x = 0)$ yp_y plane for the Hénon–Heiles model with $E = 0.16666$. All of the KAM tori have dissolved and a single chaotic trajectory wanders throughout almost all the allowed region of phase space.

Let us summarize what we have seen with the Hénon–Heiles model. For low values of the energy, most of the trajectories are associated with quasi-periodic trajectories (KAM tori). Chaotic behavior is present, but it is barely noticeable because it is confined to very small regions of phase space. As the energy increases, the KAM tori begin to dissolve via archipelago formation. The chaotic regions begin to expand. However, for a two-degree-of-freedom system, the remaining KAM tori prevent a given chaotic trajectory from wandering over the entire allowed region of phase space. After the last KAM torus (associated with the Golden Mean winding number) has disappeared, a single chaotic trajectory covers almost the entire allowed region of phase space as shown in Fig. 8.15.

Fig. 8.15. A Poincaré section $(x = 0)$ yp_y plane for the Hénon–Heiles model with $E = 0.16666$. All of the KAM tori have dissolved and a single chaotic trajectory wanders throughout almost all the allowed region of phase space.

Classificazione dei Sistemi Dinamici

Sistemi dinamici continui (Flussi)

$$\dot{X} = f(X)$$

Sistemi dinamici discreti (Mappe)

$$x_{n+1} = Ax_n(1-x_n) \equiv f_A(x)$$

Flussi Dissipativi

Flussi Hamiltoniani

Mappe Dissipative

Mappe Conservative (area-preserving)

Attrattori

1D

2D

3D

Punto fisso

Ciclo Limite

Caotici

Orbite

Periodiche

Quasi Periodiche

Caotiche

Attrattori

Punto fisso

Ciclo Limite

Caotici

Orbite

Periodiche

Quasi Periodiche

Caotiche

Classificazione dei Sistemi Dinamici

Sistemi dinamici continui (Flussi)

$$\dot{X} = f(X)$$

Sistemi dinamici discreti (Mappe)

$$x_{n+1} = Ax_n(1 - x_n) \equiv f_A(x)$$

Flussi Dissipativi

Flussi Hamiltoniani

Mappe Dissipative

Mappe Conservative (area-preserving)

Attrattori

Orbite

Attrattori

Orbite

1D

2D

3D

Punto fisso

Ciclo Limite

Caotici

Periodiche

Quasi Periodiche

Caotiche

Punto fisso

Ciclo Limite

Caotici

Periodiche

Quasi Periodiche

Caotiche

MAPPA STANDARD

Spazio-delle-fasi

SETUP

GO

SETUP-NEW-IC

K 0.93

iteration
27877

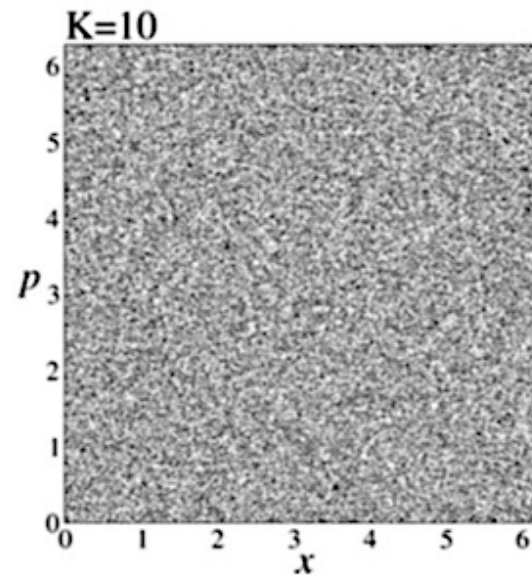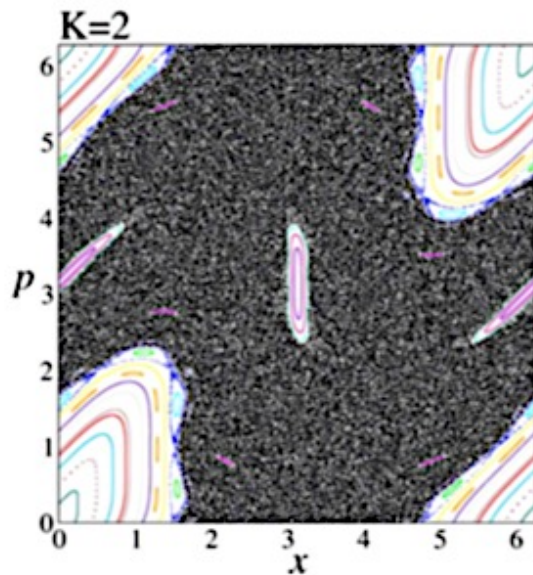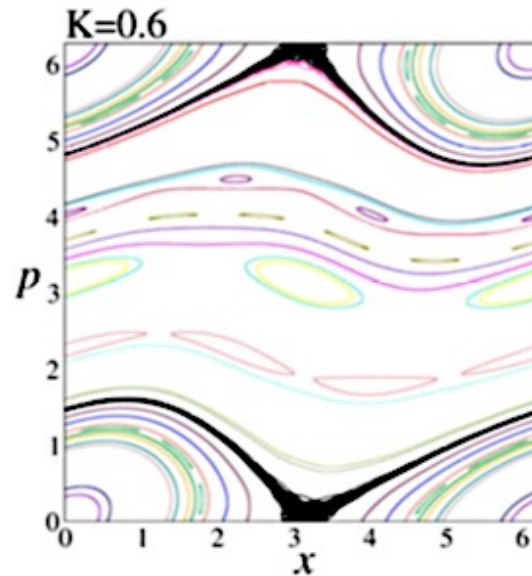$$p_{i+1} = p_i - K\sin x_i$$

$$x_{i+1} = x_i + p_{i+1}$$

where p and x are taken as modulo 2π.

Kicked Rotator

MAPPA STANDARD

K=0.2

K=0.6

K=2

K=10

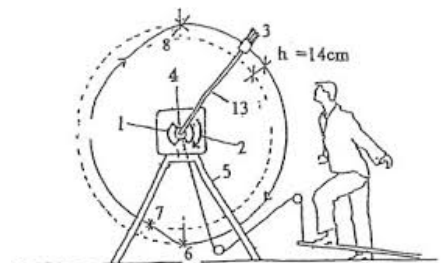SETUP

GO

SETUP-NEW-IC

K   0.93

iteration
27877

$$p_{i+1} = p_i - K\sin x_i$$

$$x_{i+1} = x_i + p_{i+1}$$

where p and x are taken as modulo 2π.

Kicked Rotator